
TOWARDS FEDERATED LEARNING ON TIME-EVOLVING HETEROGENEOUS DATA

YongXin Guo *
CUHK (SZ), P.R. China
yongxinguo@link.cuhk.edu.cn

Tao Lin *
Westlake University, P.R. China
lintao@westlake.edu.cn

Xiaoying Tang
CUHK (SZ), P.R. China
xiaoyingtang@cuhk.edu.cn

ABSTRACT

Federated Learning (FL) is a learning paradigm that protects privacy by keeping client data on edge devices. However, optimizing FL in practice can be difficult due to the diversity and heterogeneity of the learning system. Despite recent research efforts to improve the optimization of heterogeneous data, the impact of time-evolving heterogeneous data in real-world scenarios, such as changing client data or intermittent clients joining or leaving during training, has not been studied well.

In this work, we propose Continual Federated Learning (CFL), a flexible framework for capturing the time-evolving heterogeneity of FL. CFL can handle complex and realistic scenarios, which are difficult to evaluate in previous FL formulations, by extracting information from past local data sets and approximating local objective functions. We theoretically demonstrate that CFL methods have a faster convergence rate than FedAvg in time-evolving scenarios, with the benefit depending on approximation quality. Through experiments, we show that our numerical findings match the convergence analysis and that CFL methods significantly outperform other state-of-the-art FL baselines.

1 Introduction

Federated Learning (FL) has recently emerged as a critical distributed machine learning paradigm to preserve user/client privacy. Clients engaged in the training process of FL only communicate their local model parameters, rather than their private local data, with the central server.

As the workhorse algorithm in FL, FedAvg (McMahan et al., 2017) performs multiple local stochastic gradient descent (SGD) updates on the available clients before communicating with the server. Despite its success, FedAvg suffers from the large heterogeneity (non-iid-ness) in the data presented on the different clients, causing drift in each client’s updates and resulting in slow and unstable convergence (Karimireddy et al., 2020b). To address this issue, a new line of study has been suggested lately that either simulates the distribution of the whole data set using preassigned weights of clients (Wang et al., 2020; Reiszadeh et al., 2020; Mohri et al., 2019; Li et al., 2020a) or adopts variance reduction methods (Karimireddy et al., 2020b,a; Das et al., 2020; Haddadpour et al., 2021).

However, the FL formulation in these approaches always assumes a fixed data distribution among clients throughout all training rounds, while in practice this assumption does not always hold because of the complex, uncontrolled, and unpredictable client behaviors. Local data sets, for example, often vary over time, and intermittent clients can join or depart during training without prior notice. As shown in Figure 1, the local distribution of one client can also change significantly for different rounds.

The difficulty in addressing the time-evolving heterogeneity of FL lies in the stateless nature of the local data sets, which includes the unpredictable future data sets and the impossibility of retaining all prior local data sets. To this end, we first provide a novel Continual Federated Learning (CFL) formulation and then propose a unified CFL framework as our solution. This framework encompasses a variety of design choices for approximating the local objective functions in the previous training rounds, with the difference between actual and estimated local object functions described as *information loss* for further analysis.

*Equal contribution.

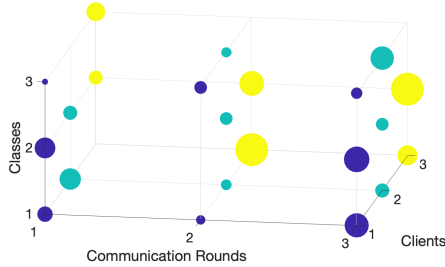


Figure 1: Time-varying heterogeneous local data distributions. The size of each ball represents the number of samples that correspond to the class. Different colors represent different clients.

To capture the time-evolving data heterogeneity in the CFL framework, we expand the theoretical assumption on the client drift—which has been extensively utilized recently in previous studies (Karimireddy et al., 2020b; Khaled et al., 2020; Li et al., 2020b)—to include both client drift and *time drift*. This allows us to quantify the difference between local client objective function and global objective function for the considered time-evolving heterogeneous clients.

We provide convergence rates for our unified CFL framework in conjunction with information loss and new models of both client and time drifts. Our analysis reveals a faster convergence of CFL framework than FedAvg (under time-evolving scenario), with the benefit dependent on approximation accuracy. The rate of CFL can simply recover the rate of FedAvg (under traditional FL scenario) and Continual Learning: the rates of FedAvg obtained from our framework is consistent with previous work, while a similarly simplified rate on Continual Learning (CL) (French, 1999; Kirkpatrick et al., 2017) is novel. Finally, in extensive empirical results, we demonstrate that CFL methods—stemmed from the CFL framework with different approximation techniques—significantly outperform the SOTA FL competitors on various simulation data sets and realistic data sets for FL settings with time-evolving heterogeneous data. These numerical observations corroborate our theoretical findings.

We summarize our key contributions:

- We present a unified framework, termed Continual Federated Learning (CFL), together with a novel client and time drift modeling approach, to capture complex FL scenarios involving time-evolving heterogeneous data, including standard cross-device FL scenario, stateless scenario, and local data set overlapping. This is the first theoretical study, to our knowledge, that describes the time-evolving nature of FL.
- We provide rigorous convergence analysis for the CFL methods. Our theoretical analysis explains the faster and more stabilized optimization of the CFL methods over that of FedAvg under time-evolving scenarios, and conjecture their variance reduction effect. In addition, we provide tight convergence rates for standalone CL methods: to the best of our knowledge, we are the first to provide such guarantees for CL on SGD.
- We thoroughly examining some conventional CL methods under the scope of CFL framework: the insights therein offer a valuable practical guideline. We believe filling such gaps is valuable to the FL community and has not been done yet. We demonstrate the efficacy and necessity of CFL methods over the SOTA FL baselines across a range of time-evolving heterogeneous data scenarios and data sets.

2 Related Work

2.1 Federated Learning

FedAvg (McMahan et al., 2017; Lin et al., 2020b) is the de facto standard FL algorithm, in which multiple local SGD steps are executed on the available clients to alleviate the communication bottleneck. While communication efficient, heterogeneity, such as system heterogeneity (Li et al., 2018; Wang et al., 2020; Mitra et al., 2021; Diao et al., 2021) and statistical/objective heterogeneity (Li et al., 2018; Wang et al., 2020; Mitra et al., 2021; Lin et al., 2020a; Karimireddy et al., 2020b,a), results in inconsistent optimization objectives and drifted clients models, impeding federated optimization considerably.

A line of work has been proposed to address the heterogeneity in FL. FedProx (Li et al., 2018) adds the regularization term on the distance of local and global models when performing local training—similar formulations can be found in other recent FL works (Hanzely & Richtárik, 2020; Dinh et al., 2020; Li et al., 2021) for various purposes. To address the issue of objective heterogeneity e.g. caused by heterogeneous data, works like SCAFFOLD (Karimireddy et al., 2020b; Mitra et al., 2021) introduce the idea of variance reduction on the client local update steps. FedNova (Wang et al., 2020)

further proposes a general framework for unifying FedAvg and FedProx, and argues that while averaging, local updates should be normalized to minimize heterogeneity induced by different number of local update steps. However, most of these prior works focus on the fixed heterogeneity across clients and throughout the entire optimization procedure; we instead consider the novel scenario with time-evolving data heterogeneity.

The theoretical study on the convergence of FedAvg can date back to the parallel SGD analysis on the identical functions (Zinkevich et al., 2010) and recently is improved by Stich (2019); Stich & Karimireddy (2020); Patel & Dieuleveut (2019); Khaled et al. (2020); Woodworth et al. (2020b). For the analysis of heterogeneous data, Li et al. (2020b) first give the convergence rate of FedAvg on non-iid data sets with random selection, assuming that the client optimum are ϵ -close. Recent studies (Woodworth et al., 2020a; Khaled et al., 2020) give tighter convergence rates under the assumption of bounded gradient drift. All above works give a $\mathcal{O}(1/T)$ convergence rate for convex local objective functions. More recently, a series of works (Karimireddy et al., 2020b; Koloskova et al., 2020) give the convergence analysis of local SGD for non-convex objective functions under bounded gradient noise assumptions, and obtain a $\mathcal{O}(1/\sqrt{T})$ convergence rate. Our theoretical analysis framework covers more challenging time-evolving data heterogeneity in FL, which has not been considered in the community yet—our rate can be simplified to the standard FL scenario, matching the tight analysis in previous works (Karimireddy et al., 2020b).

2.2 Continual Learning

Continual learning, also known as incremental learning or lifelong learning, aims to learn from (time-evolving) sequential data while avoiding the problem of *catastrophic forgetting* (French, 1999; Kirkpatrick et al., 2017). There exists a large amount of works, from the perspectives of regularization (Kirkpatrick et al., 2017; Li & Hoiem, 2017; Zenke et al., 2017), experience replay (Castro et al., 2018; Rebuffi et al., 2017), and dynamic architectures (Maltoni & Lomonaco, 2019; Rusu et al., 2016). In this paper, we examine both regularization and experience replay based methods, and compare their empirical performance in depth.

Despite the empirical success, the theoretical analysis of CL is limited: only a recent preprint (Yin et al., 2020b) provides a viewpoint of regularization-based continual learning, and only for the single worker scenario. In this work, we provide tight convergence analysis for both CL and CFL on SGD.

2.3 Continual Federated Learning

To our knowledge, the scenario of CFL was originally described in Bui et al. (2018) in order to federated train Bayesian Neural Network and continually learn for Gaussian Process models—it is orthogonal to our optimization aspect in this paper. FedCurv (Shoham et al., 2019) blends EWC (Kirkpatrick et al., 2017) regularization with FedAvg, and empirically shows a faster convergence. FedWeIT (Yoon et al., 2021) extends the regularization idea, with a focus on selective inter-client knowledge transfer for task-adaptive parameters. In another study, Zhu et al. (2021) investigate task-specific parameters and only considers the scenario in which data undergo periodic changes. In a very recent parallel (and empirical) work, CDA-FedAvg (Casado et al., 2021) uses locally maintained long-term data samples, with asynchronous communication. FLwF-2T (Usmanova et al., 2021) employs a distillation-based approach and focuses on class incremental scenarios. In Xu et al. (2022), a distillation-based method is utilized, incorporating augmented data for distillation. FedDrift (Jothimurugesan et al., 2022) focuses on the concept drift problem and proposes a multi-model approach to address it. Our theoretically sound CFL framework covers the regularization component of FedCurv and the core set part of CDA-FedAvg, and is orthogonal to the neural architecture manipulation idea in FedWeIT.

3 Continual Federated Learning Framework

3.1 Formulation

3.1.1 Conventional FL Formulation

The standard FL typically considers a sum-structured distributed optimization problem as below

$$f^* = \min_{\omega \in \mathbb{R}^d} \left[f(\omega) := \sum_{i=1}^N p_i f_i(\omega) \right], \quad (1)$$

where the objective function $f(\omega) : \mathbb{R}^d \rightarrow \mathbb{R}$ is the weighted sum of the local objective functions $f_i(\omega) := \mathbb{E}_{\mathcal{D}_i} [F_i(\omega)]$ of N nodes/clients, and p_i is the weight of client i .

In practice, it may be infeasible to select all clients each round, especially for cross-device setup (McMahan et al., 2017; Kairouz et al., 2019). The standard FedAvg then randomly selects S clients to receive the model parameters from the server ($S \leq N$) in each communication round and performs K local SGD update steps in the form of $\omega_{t,i,k} =$

Algorithm 1 Approximated CFL Framework

Require: initial weights ω_0 , global learning rate η_g , local learning rate η_l , number of training rounds T .

Ensure: trained weights ω_T .

```
1: for round  $t = 1, \dots, T$  do
2:   communicate  $\omega_t$  to the chosen clients.
3:   for client  $i \in \mathcal{S}_t$  in parallel do
4:     initialize local model  $\omega_{t,i,0} = \omega_t$ .
5:     for  $k = 1, \dots, K$  do
6:       Calculate stochastic gradient  $\tilde{g}_{t,i,k}$  by (3).
7:        $\omega_{t,i,k} \leftarrow \omega_{t,i,k-1} - \eta_l \tilde{g}_{t,i,k}$ .
8:       communicate  $\Delta\omega_{t,i} \leftarrow \omega_{t,i,K} - \omega_t$ .
9:    $\Delta\omega_t \leftarrow \frac{\eta_g}{S} \sum_{i \in \mathcal{S}_t} \Delta\omega_{t,i}$ .
10:   $\omega_{t+1} \leftarrow \omega_t + \Delta\omega_t$ .
```

$\omega_{t,i,k-1} - \eta_l(\nabla f_i(\omega_{t,i,k-1}) + \nu_{t,i,k-1})$, with local step-size η_l and gradient noise $\nu_{t,i,k-1}$. The selected clients then communicate the updates $\Delta\omega_{t,i} = \omega_{t,i,K} - \omega_t$ with the server for the model aggregation: $\omega_{t+1} = \omega_t - \frac{\eta_g}{S} \sum_{i=1}^S \Delta\omega_{t,i}$.

3.1.2 Continual FL Formulation

Despite its wide usage, the standard FL formulation given in Equation (1) cannot properly reflect actual time-evolving scenarios, such as local data sets changing over time or intermittent clients joining or leaving during training. To address this problem, we propose the Continual Federated Learning (CFL) formulation

$$f^* = \min_{\omega \in \mathbb{R}^d} \left[f(\omega) := \sum_{t=1}^T \sum_{i \in \mathcal{S}_t} p_{t,i} f_{t,i}(\omega) \right], \quad (2)$$

where $f_{t,i}(\omega)$ represents the local objective function of client i at time t . \mathcal{S}_t is a subset of clients sampled from all clients set Ω , where $|\mathcal{S}_t| = S$. For the time-evolving scenarios, client i could have different local objective functions $f_{t,i}(\omega)$ due to the changing local data sets on different t .

3.2 Approximation of CFL

The challenge of addressing CFL formulation (Equation 2) stems from the stateless nature of the local data sets, which include unpredictable future data sets, as well as the difficulty of keeping all the previous local data sets. The original definition of CFL formulation (Equation 2) is theoretically and empirically infeasible. To handle the second case (while ignoring the intractable former), a straightforward approach is to approximate the prior local objective functions (Kirkpatrick et al., 2017; Zenke et al., 2017; Li & Hoiem, 2017), which may be accomplished by retraining information from earlier rounds in accordance with privacy protection standards. Thus, we can express the approximated CFL formulation as

$$\tilde{f}_t^* = \min_{\omega \in \mathbb{R}^d} \left[\sum_{i \in \mathcal{S}_t} p_{t,i} f_{t,i}(\omega) + \sum_{\tau=1}^{t-1} \sum_{i \in \mathcal{S}_t} p_{\tau,i} \tilde{f}_{\tau,i}(\omega) \right], \quad (3)$$

where $\tilde{f}_{t,i}(\omega)$ denotes the approximated local objective function of client i at time t . In practice, different approximation methods can be used to calculate $\tilde{f}_{\tau,i}(\omega)$, and we refer the detailed illustration and discussions of these approximation algorithms in Section 5.2, Section 5.3, and Appendix C.1.2.

We give the formal definition of CFL framework in Algorithm 1. CFL methods are a collection of methods that make use of different approximation techniques and are based on Algorithm 1. We retrieve the objective function of Continual Learning (CL) by setting $S = 1$ in (3).

Take note that in most cases, the previous local object functions cannot be properly approximated. Due to the fact that such approximation impairs optimization, we define the information loss below.

Definition 3.1 (Information Loss). *Let $\Delta_{t,i}(\omega)$ be the information loss between the approximated local objective function $\tilde{f}_{t,i}(\omega)$ and the real local objective function $f_{t,i}(\omega)$. This information loss is defined as*

$$\Delta_{t,i}(\omega) = \nabla f_{t,i}(\omega) - \nabla \tilde{f}_{t,i}(\omega). \quad (4)$$

In practice, we use $\|\Delta_{t,i}(\omega)\|_2$ to measure the information loss of different approximation methods. We show large information loss can impede the convergence theoretically (c.f. Theorem 4.1) and empirically (e.g. Figure 3 in Section 5.3).

3.3 Gradient Noise Model

To analyze Equation (3) and Algorithm 1 in-depth, we propose the Gradient Noise Model (Equation 5) to capture the dynamics of performing SGD with data heterogeneity. We first recap the standard definition of gradient noise in previous works (Sammur & Webb, 2010; Gower et al., 2019).

Gradient noise in SGD. For objective function $f(\omega)$, the gradient with stochastic noise can be defined as $\nabla f(\omega) = g(\omega) + \nu$, where $g(\omega)$ is the stochastic gradient, and ν is a zero-mean noise.

Client drift in FL. To analyze the impact of data heterogeneity, recent works (Karimireddy et al., 2020b; Khaled et al., 2020; Li et al., 2020b) similarly use the gradient noise to capture the distribution drift between local objective function and global objective function

$$\nabla f(\omega) = \nabla f_i(\omega) + \delta_i,$$

where δ_i is a zero-mean random variable which measures the gradient noise of client i .

Client drift and time drift in CFL framework. Considering the distribution drift in the dimension of client and time, we further modify the gradient noise model in FL as

$$\nabla f(\omega) = \nabla f_{t,i}(\omega) + \delta_i + \xi_{t,i}. \quad (5)$$

Here we extend the gradient noise to two terms: δ_i and $\xi_{t,i}$. δ_i is a time independent (of t), zero-mean random variable that measures the drift of client i . The zero-mean $\xi_{t,i}$ measures the drift of client i at time t : We assume a fixed underlying client distribution for each client i , and the time drift is only the additive noise for the given client drift. For each client i , a time-drift will be sampled for each time step t and added on top of the fixed client drift to capture the time-evolving nature of the clients' local data sets. Notice that the random variables are nature to be zero-mean because we assume the global objective $f(\omega) = \mathbb{E}[f_{t,i}(\omega)]$ as in most FL works (Karimireddy et al., 2020b,a; McMahan et al., 2017). We use Assumption 3 to construct the non-iidness.

Remark 3.2. *To simplify the study and address the cross-device FL settings, we assume that different $\xi_{t,i}$ are independent. A more complicated change pattern of local data may arise in cross-silo FL scenarios in terms of time-dependent $\xi_{t,i}$, resulting in overlapped local data sets. The formulation of these time-dependent scenarios would need some scenario-specific assumptions, and we give some analysis in Section 4.3. Besides, to narrow the gap, in Section 5.3, we experimentally analyze the performance of CFL approaches with overlapped time-evolving local data, and the findings are consistent with our theoretical analysis.*

3.4 Assumptions

To ease the theoretical analysis of CFL (Equation 2) framework, we use the following widely used assumptions.

Assumption 1 (Smoothness and convexity). *Assume local objective functions $f_{t,i}(\omega)$ are L -smooth and μ -convex. This means that the following inequality holds for all ω_1, ω_2 : $\frac{\mu}{2} \|\omega_1 - \omega_2\|^2 \leq f_{t,i}(\omega_1) - f_{t,i}(\omega_2) - \langle \nabla f_{t,i}(\omega_2), \omega_1 - \omega_2 \rangle \leq \frac{L}{2} \|\omega_1 - \omega_2\|^2$.*

A widely used corollary is that if a function $f_{t,i}$ is both L -smooth and μ -convex, then it satisfies $\frac{1}{2L} \|\nabla f_{t,i}(\mathbf{x}) - \nabla f_{t,i}(\mathbf{y})\|^2 \leq f_{t,i}(\mathbf{x}) - f_{t,i}(\mathbf{y}) - \nabla f_{t,i}(\mathbf{x})^T (\mathbf{x} - \mathbf{y})$, and $L \geq \mu$.

Assumption 2 (Bounded noise in stochastic gradient). *Let $g_{t,i,k}(\omega) = \nabla f_{t,i,k}(\omega) + \nu_{t,i,k}$, where $\nu_{t,i,k}$ is the stochastic noise of client i on round t at k -th local update step. We assume that $\mathbb{E}[\nu|\omega] = 0$, and $\mathbb{E}[\|\nu\|^2|\omega] \leq \sigma^2$.*

Assumption 1 and 2 are common assumptions in FL (Karimireddy et al., 2020b; Li et al., 2020b). A relaxed assumption, such as bounded noise at the optimum, as discussed in recent works (Khaled et al., 2020), is an interesting direction for future research. Besides, we introduce the following assumptions to better characterize the client and time drifts in CFL framework (Equation 5).

Assumption 3 (Bounded gradient drift of CFL framework). *Let $f(\omega) = \nabla f_{t,i}(\omega) + \delta_i + \xi_{t,i}$, where δ_i independent on client i measures client drift, and $\xi_{t,i}$ independent on time t and indicates the time drift of $\{t, i\}$. We assume that $\mathbb{E}[\delta|\omega] = 0$, $\mathbb{E}[\xi|\omega] = 0$, and thus $\mathbb{E}[\|\delta\|^2|\omega] \leq G^2 + B^2\mathbb{E}\|\nabla f(\omega)\|^2$ and $\mathbb{E}[\|\xi\|^2|\omega] \leq D^2 + A^2\mathbb{E}\|\nabla f(\omega)\|^2$.*

Assumption 3 assumes the bounded $\mathbb{E}[\|\delta\|^2|\omega]$ and $\mathbb{E}[\|\xi\|^2|\omega]$ in CFL framework, which is equivalent to the widely used (G, B) gradient drift assumption² (Gower et al., 2019; Karimireddy et al., 2020b) on the bounded $\mathbb{E}[\|\nabla f_i(\omega)\|^2]$.

²The (G, B) gradient drift: $\mathbb{E}[\|\nabla f_i(\omega)\|^2] \leq G^2\mathbb{E}[\|\nabla f(\omega)\|^2] + B^2$, where $G^2 \geq 1$ and $B^2 \geq 0$.

| Algorithm | | Strongly Convex | General Convex |
|-----------|--|---|---|
| SGD | | $\frac{\sigma^2}{\mu N K \epsilon} + \frac{1}{\mu}$ | $\frac{\sigma^2}{N K \epsilon^2} + \frac{1}{\epsilon}$ |
| FedAvg | Li et al. (2020b) | $\frac{\sigma^2}{\mu^2 N K \epsilon} + \frac{(G^2 + D^2)K}{\mu^2 \epsilon}$ | - |
| | Khaled et al. (2020) | $\frac{\sigma^2 + G^2 + D^2}{\mu N K \epsilon} + \frac{\sigma + G + D}{\mu \sqrt{\epsilon}} + \frac{N(A^2 + B^2)}{\mu}$ | $\frac{\sigma^2 + G^2 + D^2}{N K \epsilon^2} + \frac{\sigma + G + D}{\mu \epsilon^{\frac{3}{2}}} + \frac{N(A^2 + B^2)}{\epsilon}$ |
| | Karimireddy et al. (2020b) | $\frac{\sigma^2}{\mu N K \epsilon} + \frac{G + D}{\mu \sqrt{\epsilon}} + \frac{c_{p_B}}{\mu}$ | $\frac{\sigma^2}{K N \epsilon^2} + \frac{G + D}{\epsilon^{\frac{3}{2}}} + \frac{c_{p_B}(D^2 + G^2)}{\epsilon}$ |
| | Woodworth et al. (2020a) | $\frac{\sqrt{c_{p_B}}}{K \sqrt{\mu \epsilon}} + \frac{\sigma^2 c_{p_B}}{N K \epsilon^2} + \frac{G + D}{\mu \sqrt{\epsilon}} + \frac{\sigma}{\mu \sqrt{K \epsilon}}$ | $\frac{c_{p_B}}{K \epsilon} + \frac{\sigma^2 c_{p_B}}{N K \epsilon^2} + \frac{(G + D)c_{p_B}}{\epsilon^{\frac{3}{2}}} + \frac{\sigma c_{p_B}}{\sqrt{K \epsilon^{\frac{3}{2}}}}$ |
| Ours | $\frac{\sigma^2}{\mu N K \epsilon} + \frac{G^2 + D^2}{\mu \epsilon} + \frac{c_{p_B}}{\mu}$ | $\frac{c_{p_B}}{\epsilon} + \frac{\sigma^2}{N K \epsilon^2} + \frac{G^2 + D^2}{\epsilon^2}$ | |
| CL | Yin et al. (2020b) | $\frac{\mu}{\epsilon} \text{ (GD)}$ | - |
| | Ours | $\frac{1 + A^2}{\mu} + \frac{\sigma^2}{\mu K \epsilon} + \frac{c_A}{\mu \epsilon}$ | $\frac{c_{p_B}}{\epsilon} + \frac{\sigma^2}{K \epsilon^2} + \frac{c_A}{\epsilon^2}$ |
| CFL | Ours | $\frac{c_{p_B}}{\mu} + \frac{\sigma^2}{\mu N K \epsilon} + \frac{c_A + G^2}{\mu \epsilon}$ | $\frac{c_{p_B}}{\epsilon} + \frac{\sigma^2}{N K \epsilon^2} + \frac{c_A + G^2}{\epsilon^2}$ |

Table 1: Number of communication rounds required to reach $\epsilon + \varphi$ accuracy for μ strongly convex and general convex functions under time-evolving FL scenarios (Assumption 1–4). We can recover the rates in conventional FL setups by setting $D = 0$ and $A = 0$. Note that $\varphi = 0$ in FedAvg. Our convergence rate of FedAvg matches the results in previous works (Karimireddy et al., 2020b). Our SGD rate of CL on the strongly-convex case is novel. Note that all elaborated results use SGD unless specifically mentioned. $c_{p_B} = 1 + B^2 + A^2$, $c_A = \frac{D^2 R^2}{R^2 + D^2}$. N is the number of chosen clients in each round, and K is the number of local iterations.

We prove this claim in Appendix B.1. Notice that when $D > 0$, or $G > 0$, the clients’ local optimum at round t , $\omega_{i,t}^*$ will be different from global optimum ω^* . Besides, as illustrated before, $\mathbb{E}[\delta|\omega] = 0$ and $\mathbb{E}[\xi|\omega] = 0$ are nature due to the assumption of global objective $f(\omega) = \mathbb{E}[f_{t,i}(\omega)]$ as in most FL works (Karimireddy et al., 2020b,a; McMahan et al., 2017).

Assumption 4 (Bounded information loss). *Let R be a non-negative real number and ω be a vector. We assume that the information loss $\Delta_{t,i}(\omega)$ satisfies $|\Delta_{t,i}(\omega)| \leq R$.*

Remark 3.3. *In Assumption 4, the exact information loss may be difficult to calculate for certain approximation methods, such as generative replay. In Lemma B.3 of Appendix B.3, we provide a detailed analysis of information loss for Taylor extension based regularization methods and provide a more general case in the main paper.*

4 Theoretical results

In this section, we analyze the theoretical performance of Algorithm 1 under Assumption 1–4. We prove that CFL methods converges faster than FedAvg, despite that the term (refer to φ in Theorem 4.1, which is a bias term that can not eliminate by reducing learning rate) induced by information loss concurrently trades off the optimization. Additionally, our results include the FedAvg rate (and match the prior work) and a novel convergence rate for SGD on CL. In Table 1, we summarize the convergence rate of different algorithms³. The proof details refer to Appendix B.4 and Appendix B.5.

4.1 Convergence Rate of CFL Methods

Before analyzing Algorithm 1, we want to clarify that the introduced information loss $\Delta_{t,i}$, which is an approximation error, will introduce a constant that cannot be eliminated by reducing the learning rate. Therefore, instead of aiming for convergence to an arbitrary ϵ , we aim to optimize until the expected error is smaller than $\epsilon + \varphi$, where $\varphi = \frac{\sum_{t=1}^T q_t \varphi_t}{\sum_{t=1}^T q_t}$ for some sequence q_t and constant φ_t . The value of φ_t is positively related to the bounded information loss R defined in Assumption 4. Details of the proof can be found in Appendix B.4.

Theorem 4.1 (Convergence rate of CFL methods). *Assume $\{f_{t,i}(\omega)\}$ satisfy Assumption 1–4, the output of Algorithm 1 has expected error smaller than $\epsilon + \varphi$, for $\eta_g = 1$, $\eta_l \leq \frac{\sqrt{3+4(1+B^2+A^2)} - \sqrt{4(1+B^2+A^2)}}{6KL\sqrt{1+B^2+A^2}}$, $p_{\tau,i} = \frac{D^2}{tD^2+(t-1)R^2}$ ($\tau < t$), and $p_{t,i} = \frac{(t-1)R^2+D^2}{tD^2+(t-1)R^2}$ on round t .*

³To match the notations of prior works that include all clients in all training rounds, we use the abbreviation N to denote the number of selected clients in each round in this section.

When $\{f_{t,i}(\omega)\}$ are μ -strongly convex functions, we have

$$T = \mathcal{O} \left(\frac{Lc_O}{\mu} + \frac{\sigma^2}{\mu NK\epsilon} + \frac{1}{\mu\epsilon} \left(G^2 + \frac{D^2 R^2}{R^2 + D^2} \right) \right),$$

and when $\{f_{t,i}(\omega)\}$ are general convex functions ($\mu = 0$), we have

$$T = \mathcal{O} \left(\frac{c_O \mathcal{H}}{\epsilon} + \frac{\sigma^2 \mathcal{H}}{NK\epsilon^2} + \frac{\mathcal{H}}{\epsilon^2} \left(G^2 + \frac{D^2 R^2}{R^2 + D^2} \right) \right),$$

and when $\{f_{t,i}(\omega)\}$ are non-convex, setting $\eta = K\eta_g\eta_l = \frac{\sqrt{KN}}{\sqrt{TL}}$, when $\frac{1}{T} \sum_{t=1}^T \mathbb{E} \left[\|\nabla f(\omega_t)\|^2 \right]$ reach ϵ we have

$$T = \mathcal{O} \left(\frac{L^2(f_0 - f_*)^2}{NKc_m^2\epsilon^2} + \frac{1}{\epsilon^2} \left(\frac{\sqrt{KN}c_{R1}^2}{L} + \frac{\sigma^2}{\sqrt{NK}} \right)^2 \right),$$

where $c_O = 1 + A^2 + B^2$, $c_{R1} = \frac{R^2}{R^2 + D^2}$, c_m is a constant related to A , B and R , and $\mathcal{H} = \|\omega_0 - \omega^*\|^2$. N is the number of chosen clients in each round, and K is the number of local iterations. We elaborate the choice of $p_{t,i}$ in Appendix B.4.3.

Remark 4.2. When setting $N = 1$ in Theorem 4.1, we recover the convergence rate of standalone CL methods. To the best of our knowledge, we are the first to provide such theoretical guarantees for SGD: the recent work (Yin et al., 2020a) only gives the convergence rate of GD for regularization based CL methods on general convex case, under the constraint of information loss $R = 0$.

Proposition 4.3. For stateless cross-device FL scenarios (clients only appear once during training), we can derive lower bounds than that of Theorem 4.1. More precisely, by applying Lemma B.2 to the considered stateless scenario, the key variance term $c_{normal} = G^2 + \frac{D^2 R^2}{R^2 + D^2}$ in Theorem 4.1 becomes $c_{stateless} = \frac{(G^2 + D^2)R^2}{G^2 + D^2 + R^2}$. $c_{stateless}$ is the lower bound of c_{normal} , indicating that CFL methods provide higher performance improvements in stateless FL scenarios.

4.2 Convergence Rate of FedAvg under Time-evolving Scenarios

To show the faster convergence of CFL methods than FedAvg, we provide the convergence rate of FedAvg under time-evolving scenarios and Assumption 1–4. Note that prior works only consider traditional FL scenarios (w/o time-evolving heterogeneous data) for FedAvg, and we offer new rates of FedAvg for such scenarios by setting $p_{t,i} = 1$.

Theorem 4.4 (Convergence rate of FedAvg under time-evolving scenarios). Assume $\{f_{t,i}(\omega)\}$ satisfy Assumption 1–4, the output of FedAvg has expected error smaller than ϵ , for $\eta_g = 1$ and $\eta_l \leq \frac{\sqrt{3+4(1+B^2+A^2)} - \sqrt{4(1+B^2+A^2)}}{6KL\sqrt{1+B^2+A^2}}$. When $\{f_{t,i}(\omega)\}$ are μ -strongly convex functions, we have

$$T = \mathcal{O} \left(\frac{Lc_O}{\mu} + \frac{\sigma^2}{\mu NK\epsilon} + \frac{G^2 + D^2}{\mu\epsilon} \right),$$

and when $\{f_{t,i}(\omega)\}$ are general convex functions ($\mu = 0$), we have

$$T = \mathcal{O} \left(\frac{c_O \mathcal{H}}{\epsilon} + \frac{\sigma^2 \mathcal{H}}{NK\epsilon^2} + \frac{(G^2 + D^2)\mathcal{H}}{\epsilon^2} \right),$$

and when $\{f_{t,i}(\omega)\}$ are non-convex, setting $\eta = K\eta_g\eta_l = \frac{\sqrt{KN}}{\sqrt{TL}}$, when $\frac{1}{T} \sum_{t=1}^T \mathbb{E} \left[\|\nabla f(\omega_t)\|^2 \right]$ reach ϵ we have

$$T = \mathcal{O} \left(\frac{L^2(f_0 - f_*)^2}{NKc_m^2\epsilon^2} + \frac{1}{\epsilon^2} \left(\frac{\sqrt{KN}}{L} + \frac{\sigma^2}{\sqrt{NK}} \right)^2 \right),$$

where $c_O = 1 + A^2 + B^2$, and $\mathcal{H} = \|\omega_0 - \omega^*\|^2$. N is the number of chosen clients in each round, and K is the number of local iterations.

Note that in both Theorem 4.1 and Theorem 4.4, we only elaborate dominate terms to clarify the difference. Details please refer to Theorem B.5 and B.6 in Appendix B.6.

Remark 4.5. FedAvg (under time-evolving scenarios) is a special case of CFL methods by setting $p_{t,i} = 1$, as stated in Theorem 4.1 and Theorem 4.4. We show in Appendix B.4 that the rate of FedAvg (under time-evolving scenarios) is equivalent to setting the upper bound of information loss $R \rightarrow \infty$. Similar observations can be found by setting $R \rightarrow \infty$ in $p_{t,i} = \frac{(t-1)R^2 + D^2}{tD^2 + (t-1)R^2}$ in Theorem 4.1.

Remark 4.6. CFL methods accelerate the convergence by reducing the variance term of FedAvg. For example, the gradient noise term $G^2 + D^2$ of FedAvg for convex functions in Theorem 4.4 can be decreased to $G^2 + \frac{D^2 R^2}{R^2 + D^2}$ in Theorem 4.1. Similarly, the gradient noise term of non-convex functions can be reduced from 1 to $\frac{R^2}{R^2 + D^2}$. The benefits of variance reduction in CFL depend on the approximation accuracy R , as stated in remark 4.5.

4.3 Discussion: Convergence Rate of CFL for Time-dependent Drifts

In the previous sections, our convergence rates—though valuable—only assume a time t independent time drift $\xi_{t,i}$ (c.f. Assumption 3), an assumption may not always hold in practice. In this section, we extend our convergence analysis of CFL to the correlated time drifts.

Assumption 5 (Correlated time drifts). *Let $\xi_{t_1,i}$ and $\xi_{t_2,i}$ be time drifts of client i at times t_1 and t_2 , respectively. We assume that the expected value of the correlation between $\xi_{t_1,i}$ and $\xi_{t_2,i}$ given ω satisfies $\mathbb{E}[\langle \xi_{t_1,i}, \xi_{t_2,i} \rangle | \omega] \leq F_{t_1,t_2}^2 + C_{t_1,t_2}^2 \mathbb{E}[\|\nabla f(\omega)\|^2]$.*

Assumption 5 assumes that time drifts $\xi_{t_1,i}$ and $\xi_{t_2,i}$ are correlated, which allows us to simulate more complex scenarios by setting different relationships between $F_{t_1,i}$ and $F_{t_2,i}$ (also $C_{t_1,i}$ and $C_{t_2,i}$). In the following subsections, we present two case studies to examine time drifts in real-world scenarios.

4.3.1 Case 1

In the first case, we consider the following scenario: Local data sets in different rounds have overlap. Then we assume the bounded correlation between time drifts in the following assumption.

Assumption 6 (Correlated time drifts: Case 1). *Let $\xi_{t_1,i}$ and $\xi_{t_2,i}$ be time drifts of client i at times t_1 and t_2 , respectively. We assume that the expected value of the correlation between $\xi_{t_1,i}$ and $\xi_{t_2,i}$ given ω satisfies $\mathbb{E}[\langle \xi_{t_1,i}, \xi_{t_2,i} \rangle | \omega] \leq F^2 + C^2 \mathbb{E}[\|\nabla f(\omega)\|^2]$.*

Assumption 6 states that the correlation between these time drifts is bounded by constants F and C . This is a generalized assumption when the change in time drifts over time is unknown, and we use the same F and C for all t_1, t_2 in Assumption 5. For instance, in stateless FL, servers may not have information on the overlap of new clients with clients in previous rounds. Under this more realistic assumption, we provide the convergence rate of CFL.

Theorem 4.7 (Convergence rate of CFL methods with correlated time drifts). *Assume $\{f_{t,i}(\omega)\}$ satisfy Assumption 1–6, the output of Algorithm 1 has expected error smaller than $\epsilon + \varphi$, for $\eta_g = 1$, $\eta_l \leq \frac{\sqrt{3+4c_O} - \sqrt{4c_O}}{6KL\sqrt{c_O}}$, $p_{\tau,i} = \frac{M^2}{t(M^2) + (t-1)R^2}$ (for $\tau < t$), and $p_{t,i} = \frac{(t-1)R^2 + M^2}{t(M^2) + (t-1)R^2}$ on round t .*

When $\{f_{t,i}(\omega)\}$ are μ -strongly convex functions, we have

$$T = \mathcal{O} \left(\frac{Lc_O}{\mu} + \frac{\sigma^2}{\mu NK\epsilon} + \frac{1}{\mu\epsilon} \left(G^2 + \frac{M^2 R^2}{R^2 + M^2} \right) \right),$$

and when $\{f_{t,i}(\omega)\}$ are general convex functions ($\mu = 0$), we have

$$T = \mathcal{O} \left(\frac{c_O \mathcal{H}}{\epsilon} + \frac{\sigma^2 \mathcal{H}}{NK\epsilon^2} + \frac{\mathcal{H}}{\epsilon^2} \left(G^2 + \frac{M^2 R^2}{R^2 + M^2} \right) \right),$$

and when $\{f_{t,i}(\omega)\}$ are non-convex, by setting $\eta = K\eta_g\eta_l = \frac{\sqrt{KN}}{\sqrt{TL}}$, $\frac{1}{T} \sum_{t=1}^T \mathbb{E}[\|\nabla f(\omega_t)\|^2]$ needs to take the following steps to reach ϵ

$$T = \mathcal{O} \left(\frac{L^2(f_0 - f_*)^2}{NKc_m^2\epsilon^2} + \frac{1}{\epsilon^2} \left(\frac{\sqrt{KN}c_{R1}^2}{L} + \frac{\sigma^2}{\sqrt{NK}} \right)^2 \right),$$

where $M^2 = \max(0, D^2 - F^2)$, $c_O = 1 + A^2 + \max(B^2, C^2)$, $c_{R1} = \frac{R^2}{R^2 + M^2}$, c_m is a constant related to A , B , C and R , and $\mathcal{H} = \|\omega_0 - \omega^*\|^2$. N is the number of chosen clients in each round, and K is the number of local iterations. We elaborate the choice of $p_{t,i}$ in Appendix B.4.3.

Remark 4.8. Comparing Theorem 4.1 and Theorem 4.7, we can see that the convergence rate of CFL with correlated time drifts is equivalent to setting the time drift D^2 to be $\max(0, D^2 - F^2)$ in Theorem 4.1. This suggests that the correlation between time drifts can reduce the impact of time drifts on the convergence rate, and the weights of previous rounds' objective function $p_{\tau,i}$ decrease as F^2 increases. This aligns with our observations in real-world settings. For instance, when local data sets contain data from previous rounds, the model performance is significantly improved (cf. Table 9). This observation also supports the effectiveness of core set based methods in Continual Learning.

4.3.2 Case 2

In the second case, we assume that local data sets change gradually over time. Specifically, the overlap between the current data set D_t and the previous data set D_τ decreases as the time difference $|t - \tau|$ increases. This leads to the extension of Assumption 5.

Assumption 7 (Correlated time drifts: Case 2). *We assume that the correlation between time drifts $\xi_{t_1,i}$ and $\xi_{t_2,i}$ decreases as $|t_1 - t_2|$ increases to model a scenario where local data sets change gradually over time. This is formalized as*

$$\mathbb{E} [\langle \xi_{t_1,i}, \xi_{t_2,i} \rangle | \omega] \leq \alpha^{|t_1 - t_2|} \left(D^2 + A^2 \mathbb{E} [\|\nabla f(\omega)\|^2] \right),$$

where $0 \leq \alpha < 1$, and D and A are constants as defined in Assumption 3.

Under Assumption 7, the correlation between ξ_τ and ξ_t increases as the absolute value of $t - \tau$ decreases. The value of α controls the rate at which local data sets change over time. A large value of α indicates a slower rate of change.

Deriving the final convergence rate for this scenario is non-trivial. Therefore, we analyze the choice of weights $p_{\tau,i}$ and provide some insights. On top of the proof stated in Section B.8, we optimize $p_{t,i}$ to minimize the upper bound of the convergence rate. Under Assumption 1–4 and Assumption 7, the optimal weights of $p_{t,i}$ can be given by

$$\begin{aligned} \min_p \frac{1}{N} \sum_{i=1}^N (1 - p_{t,i})^2 R^2 + G^2 + D^2 \sum_{\tau_1, \tau_2}^t \alpha^{\|\tau_1 - \tau_2\|} p_{\tau_1} p_{\tau_2}, \\ \text{s.t. } \sum_{\tau=1}^t p_{\tau,i} = 1, \forall i = 1, \dots, N. \end{aligned}$$

The given optimization problem can be reformulated as a quadratic programming problem and can be solved by finding the solution to the corresponding linear system.

Theorem 4.9 (Optimal choice of $p_{\tau,i}$ under correlated time drifts). *Let $f_{t,i}(\omega)$ satisfy Assumptions 1–4 and Assumption 7. On round t , the optimal choice of $\hat{p} = [p_{1,i}, \dots, p_{t,i}]^\top$ is determined by solving the linear system*

$$\begin{bmatrix} Q & \mathbf{1} \\ \mathbf{1}^\top & 0 \end{bmatrix} \begin{bmatrix} \hat{p} \\ \lambda \end{bmatrix} = \begin{bmatrix} \mathbf{0} \\ 1 \end{bmatrix}, \quad (7)$$

where each entry of $\mathbf{1} \in \mathbb{R}^t$ is 1, and λ is the Lagrange multiplier that comes out of the solution alongside \hat{p} . Matrix Q is defined as

$$Q = \begin{bmatrix} D^2 + R^2 & \alpha D^2 + R^2 & \dots & \alpha^{t-2} D^2 + R^2 & \alpha^{t-1} D^2 \\ \alpha D^2 + R^2 & D^2 + R^2 & \dots & \alpha^{t-3} D^2 + R^2 & \alpha^{t-2} D^2 \\ \vdots & \vdots & \ddots & \vdots & \vdots \\ \alpha^{t-2} D^2 + R^2 & \alpha^{t-3} D^2 + R^2 & \dots & \alpha^2 D^2 + R^2 & \alpha D^2 \\ \alpha^{t-1} D^2 & \alpha^{t-2} D^2 & \dots & \alpha D^2 & D^2 \end{bmatrix}.$$

The optimal $p_{\tau,i}$ can be found by solving the linear system in Theorem 4.9. It is easy to show that Q is positive definite (see Lemma B.9), and we can then use LU factorization to solve the linear system in Theorem 4.9.

Example 1. *Solving the linear system in Theorem 4.9 requires the values of α , D , and R . It is difficult to provide an explicit expression of $p_{t,i}$ with arbitrary α , D , and R . Therefore, we use a toy example to provide some insights. We set different values of α , D , and R ($t = 4$ for all settings) and solve the linear system in Theorem 4.9 accordingly. The results in Table 2 show that the optimal weights of the current round increase as α increases. This indicates that a larger correlation between time drifts results in lower importance of previous rounds' objectives. This aligns with our observation in Theorem 4.7 that, as the time correlation bound F^2 increases, $p_{\tau,i}$ defined in Theorem 4.7 decreases and the convergence rate in Theorem 4.7 increases, indicating that the impact of time drifts on convergence is reduced.*

5 Experiments

We utilize the Noisy Quadratic Model—a simple convex model—to verify the theoretical results presented in Section 4. The results in Appendix 5.1 demonstrate that the convergence rate of CFL methods is much faster than baselines like

Table 2: Optimal weights of CFL with correlated time drifts. We solve the optimization problem defined in Theorem 4.9 with different α , D , and R , and report the optimal p_τ for $\tau = 1, \dots, 4$.

| α | D | R | p_1 | p_2 | p_3 | p_4 |
|----------|-----|-----|--------|--------|---------|--------|
| 0 | 2 | 1 | 0.1818 | 0.1818 | 0.1818 | 0.4545 |
| 0.5 | 1 | 0.5 | 0.2857 | 0.1429 | 0.0000 | 0.5714 |
| 0.5 | 1 | 1 | 0.2632 | 0.1316 | -0.0789 | 0.6842 |
| 0.8 | 1 | 0.5 | 0.3870 | 0.0774 | -0.2077 | 0.7434 |
| 0.8 | 2 | 0.5 | 0.3960 | 0.0792 | -0.1188 | 0.6436 |

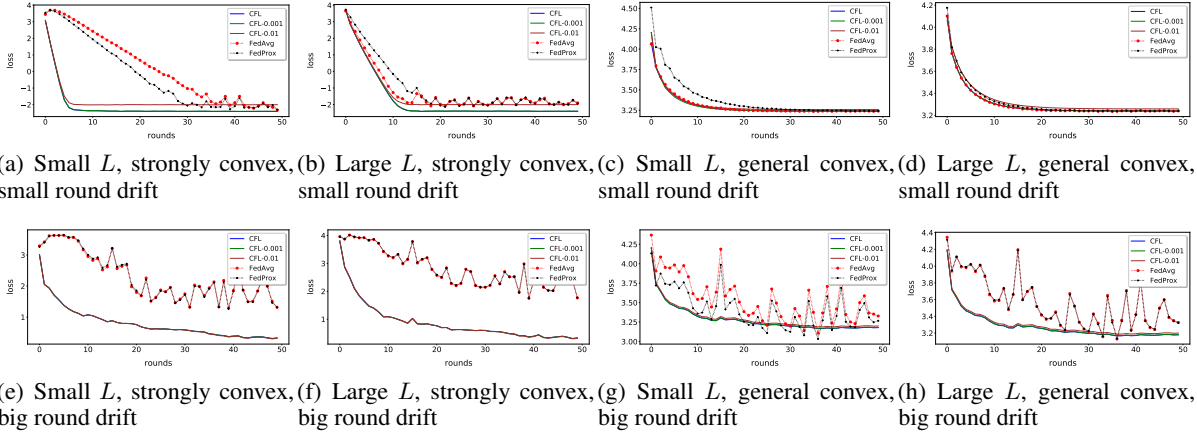


Figure 2: Performance of different algorithms on noisy quadratic model. The curves all evaluate the loss on global test data sets. We set the information loss to 0 for CFL, and CFL-0.01 and CFL-0.001 represent different levels of information loss.

FedAvg and FedProx, with a smoother convergence curve. These findings support the variance reduction effect of CFL methods mentioned in Remark 4.6.

We further conduct extensive empirical evaluations comparing the performance of our CFL methods with various strong FL competitors on a variety of realistic data sets. Additionally, we explore various approximation techniques in our CFL methods and demonstrate how they can be used to achieve efficient federated learning with time-evolving data heterogeneity.

5.1 Noisy Quadratic Model

In this section, we introduce the Noisy Quadratic Models and show the superior performance of CFL over FedAvg and FedProx (Li et al., 2018).

5.1.1 Setup of Noisy Quadratic Models

We utilize the noisy quadratic model from Zhang et al. (2019) to simulate the assumptions made in our proof. This model is defined by $f(\omega) = \omega^T \mathbf{A} \omega + \mathbf{B}^T \omega + \mathbf{C}$, where $\omega \in \mathbb{R}^n$ is the parameter we aim to optimize and $\mathbf{A} \in \mathbb{R}^{n \times n}$, $\mathbf{B} \in \mathbb{R}^n$, and $\mathbf{C} \in \mathbb{R}$ are matrices with $\mathbf{A} \succeq 0$. To construct \mathbf{A} , we first create a diagonal matrix Λ and then let $\mathbf{A} = \mathbf{U}^T \Lambda \mathbf{U}$, where \mathbf{U} is a unitary matrix. By controlling the eigenvalues of \mathbf{A} , we can control the convexity of the model, ensuring that $\mu \leq \lambda_{\min}(\mathbf{A}) \leq \lambda_{\max}(\mathbf{A}) \leq L$. Since the eigenvalues of Λ and \mathbf{A} are the same, it is simple to control the eigenvalues of \mathbf{A} by controlling those of Λ .

To simulate Assumptions 2 and 3, we introduce the gradient noise model given by

$$g_{t,i}(\omega) = \mathbf{A} \omega + \mathbf{B} + \delta_i + \xi_{t,i} + \nu_{t,i,k}, \quad \tilde{g}_{t,i}(\omega) = g_{t,i}(\omega) + \mathcal{N}(\mathbf{I}, \mathbf{I}/1000),$$

where δ_i represents the client drift of client j , $\xi_{t,i}$ denotes the round drift of client j on round i , and $\nu_{t,i,k}$ denotes the noise of gradient of client j on round i , iteration k . All of these drifts and noise are generated from a Normal distribution with zero mean and different variance. The term $\mathcal{N}(\mathbf{I}, \mathbf{I}/1000)$ is used to simulate information loss, and we use $\tilde{g}_{t,i}(\omega)$ instead of $g_{t,i}(\omega)$ in the CFL algorithm, and set different values of I to study the effect of information loss.

Table 3: Best learning rate of different algorithms on noisy quadratic model. we denote small round drift as SRD, big round drift as BRD, small L as SL, large L as LL, strongly convex as SC, and general convex as GC.

| Method | SRD | | | | BRD | | | |
|---------|-------|-------|-------|-------|-------|-------|-------|-------|
| | SL-SC | LL-SC | SL-GC | LL-GC | SL-SC | LL-SC | SL-GC | LL-GC |
| FedAvg | 0.03 | 0.08 | 0.33 | 0.09 | 0.02 | 0.01 | 0.09 | 0.02 |
| FedProx | 0.04 | 0.07 | 0.35 | 0.09 | 0.02 | 0.01 | 0.26 | 0.02 |
| CFL | 0.2 | 0.09 | 0.35 | 0.09 | 0.25 | 0.08 | 0.3 | 0.08 |

In practice, to show if the numerical results match our theoretical results, we conducted eight experiments with varying settings. We examined large and small values of L , as well as different levels of convexity and round drift. For L , we set $L = 20$ for large values and $L = 5$ for small values. For convexity, we set $\mu = 1$ for strongly convex and $\mu = 0$ for general convexity. For round drift, we set $\mathbb{E}\|\xi_{t,i}\|^2 = 100$ for large drift and $\mathbb{E}\|\xi_{t,i}\|^2 = 0.01$ for small drift. Additionally, we fixed the variance of δ_i and $\nu_{t,i,k}$ at $\mathbb{E}\|\delta_i\|^2 = 0.01$ and $\mathbb{E}\|\nu_{t,i,k}\|^2 = 0.00001$.

To perform gradient descent, we set $\omega_{t,i,k+1} = \omega_{t,i,k} - \eta l g_{t,i}(\omega_{t,i,k})$. We use the loss function $\|A\omega + B\|$ because it reaches 0 at the global optimal point for convex functions, and has a large value when far from the global optimal point.

5.1.2 Results for Noisy Quadratic Models

The results of our experiments can be found in Table 3 and Figure 2. From these results, we can draw the following conclusions:

- CFL algorithms can tolerate higher learning rates. As seen in Table 3, the best learning rates for different FL algorithms on noisy quadratic model are higher for CFL algorithms.
- CFL algorithms demonstrate better convergence than other FL baselines. From Figure 2, it is clear that CFL outperforms other FL baselines in all settings. Additionally, the loss curves of CFL are smoother, indicating a reduced variance of gradients. Furthermore, we find that the convergence of CFL with larger information loss (CFL-0.01) is worse than that of CFL with smaller information loss (CFL and CFL-0.001).

5.2 Experiments Setup for Real Datasets

Time-evolving heterogeneous local data sets. We study the use of federated learning on split-CIFAR10, split-CIFAR100, and split-Fashion-MNIST data sets for image classification tasks using ResNet18 and a two layer MLP. The split is based on the Latent Dirichlet Allocation (LDA) method, as proposed in Yurochkin et al. (2019); Hsu et al. (2019); Reddi et al. (2021), to control distribution drift with the parameter α (see Algorithm 6). Higher values of α result in smaller drifts.

Unless specifically mentioned otherwise our studies use the following protocol. All data sets are partitioned to 210 subsets for 7 distinct clients: all clients are selected and trained for 500 communication rounds, and each client randomly samples one of the corresponding 30 subsets for the local training—this challenging time-evolving scenario mimics the realistic client data sampling scheme (from some underlying distributions). Notably, the training strategy used in this section is applicable to all FL baselines and CFL methods, and we assess the model performance using a global test data set⁴. We carefully tune the hyper-parameters in all algorithms (details refer to Appendix C.1.1), and report the optimal results (i.e. mean test accuracy across the past 5 best epochs) after repeated trials.

Approximation techniques in CFL methods. Below, we review three representative types of information approximation techniques in CL, and use them to investigate the effect of various types of information loss under the (2) formulation. We refer to Appendix C.1.2 for a more comprehensive introduction and discussion.

- *Regularization methods.* Instead of keeping data sets from previous rounds, we keep track the gradients and Hessian matrices of local objective functions, and use Taylor Extension to approximate the local objective functions in previous rounds. Note that the trade-off between Hessian estimation and computational overhead constrains the practical feasibility of such approach.
- *Core set methods.* Another simple yet effective treatment in CL lines in the category of Exemplar Replay (Rebuffi et al., 2017; Castro et al., 2018). This method selects and regularly saves previous core-set samples (a.k.a. exemplars), and replays them with the current local data sets.

⁴The training loss/accuracy on (2) formulation are closely aligned with that of global test data, as shown in Figure 6 of Appendix C.1.3. We here only present the global test results for the common interests in practice.

Table 4: Top-1 accuracy for different choices of approximation techniques in CFL. We train ResNet18 on split-CIFAR10 data set (w/ $\alpha = 0.2$) for 300 communication rounds, and the data set is partitioned to 300 subsets for 10 different clients. All examined algorithms use FedAvg as the backbone.

| Algorithm | Regularization Methods | | Core Set Methods | | | | Generative Methods |
|-----------|------------------------|---------------------------|-------------------|------------------------------------|-------------------|-------------------|--------------------|
| | PyHessian | Fisher Information Matrix | Naive (Small Set) | Naive (Large Set) | iCaRL (Small Set) | iCaRL (Large Set) | MCMC |
| Accuracy | 74.15 \pm 0.66 | 73.70 \pm 0.39 | 77.84 \pm 0.06 | 78.90 \pm 0.09 | 76.97 \pm 0.16 | 77.09 \pm 0.09 | 74.18 \pm 0.08 |

Table 5: Top-1 accuracy of various CFL methods on diverse data sets for training ResNet18 with 500 communication rounds. In order to observe a noticeable performance difference on Fashion-MNIST, we use $\alpha = 0.1$ instead. All examined algorithms use FedAvg as the backbone. Both CFL-Regularization and CFL-Regularization-Full are regularization based method, and the difference lies on where the regularization is applied: the full version applies regularization to all layers while the other only considers the top layers. R_r indicates the accuracy of CFL-Regularization, while R_f denotes the accuracy of FedAvg.

| Algorithm | Accuracy on Fashion-MNIST (%) | Accuracy on CIFAR10 (%) | Accuracy on CIFAR100 (%) |
|-------------------------|------------------------------------|------------------------------------|------------------------------------|
| FedAvg | 86.75 \pm 0.14 | 70.51 \pm 0.19 | 49.97 \pm 0.19 |
| CFL-Regularization | 87.02 \pm 0.21 | 70.86 \pm 0.31 | 50.69 \pm 0.06 |
| CFL-Core-Set | 88.32 \pm 0.12 | 81.48 \pm 0.24 | 53.17 \pm 0.08 |
| CFL-Regularization-Full | 77.37 \pm 0.63 | 33.09 \pm 1.45 | 14.84 \pm 0.12 |

| Metric | Improvement on Fashion-MNIST (%) | Improvement on CIFAR10 (%) | Improvement on CIFAR100 (%) |
|-----------------------------|----------------------------------|----------------------------|-----------------------------|
| Absolute ($R_r - R_f$) | 0.27 | 0.35 | 0.72 |
| Ratio ($(R_r - R_f)/R_f$) | 0.31 | 0.50 | 1.44 |

- *Generative methods.* Maintaining a core set for each client may become impractical when learning scales to millions of clients. To ensure a privacy-preserved federated learning, the generative models (Goodfellow et al., 2014) could be used locally to capture the local data distribution: fresh data samples will be generated on the fly and combined with the current local data set. For the sake of simplicity, we use Markov Chain Monte Carlo (Nori et al., 2014) in our assessment.

5.3 Experiments Results for Real Datasets

In this section, we conduct experiments on real data sets and show the effectiveness of CFL-based methods.

5.3.1 Comments on Different CFL Approximation Techniques

In Table 4, we examine the performance of several approximation techniques using the split-CIFAR10 data set. We can conclude that

1. *Core set methods outperform other methods by a significant margin.* The simple choice of “naive core set”, i.e. randomly and uniformly sample data from the local data set, surpasses the sampling technique described in iCaRL (Rebuffi et al., 2017)⁵ for CL, despite their faster convergence in the initial training phase.
2. *The quality of Hessian estimation matters for regularization based methods.* PyHessian (Yao et al., 2020), as a method to approximate diagonal Hessian matrix, is slightly preferable than Fisher Information Matrix, though the latter one involves less computation.
3. *The performance of generative methods is restricted,* and we hypothesize that the poor quality of generated samples contributes to the constraint.

In the subsequent evaluation, we consider naive core set sampling for CFL-Core-Set method, and use PyHessian for CFL-Regularization. We exclude the results of generative methods, due to the trivial performance gain and significant computational overhead.

5.3.2 Understanding Various Approximated CFL Implementations on Different Datasets

Table 5 experimentally studies the impacts of various information approximation techniques in CFL methods—as discussed in Section 5.2—and compares them with the backbone algorithm of CFL methods, i.e. FedAvg. We have the following consistent findings on different data sets:

1. *The improvement of CFL methods over FedAvg becomes larger for more challenging tasks,* as shown in the bottom of the Table 5 for regularization based methods. This might reflect the fact that the precision of the information

⁵The algorithmic details of the sampling method in iCaRL refer to Algorithm 3 in Appendix C.1.2.

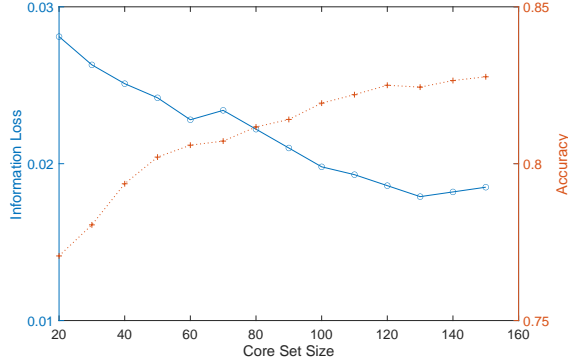


Figure 3: Information loss (left y-axis) and accuracy (right y-axis) for training ResNet18 on split-CIFAR10 with different core set sizes (x-axis) and $\alpha = 0.2$.

Table 6: Comparing the SOTA FL baselines with several CFL methods, for training ResNet18 on split-CIFAR10 data set with different degrees of non-iid-ness α (and with total 500 communication rounds).

| Accuracy | FL baselines | | | CFL methods | | |
|----------------|------------------|------------------|------------------|------------------------------------|--------------------|------------------------------|
| | FedAvg | FedProx | MimeLite | CFL-Core-Set | CFL-Regularization | CFL-Regularization + FedProx |
| $\alpha = 0.1$ | 70.51 ± 0.19 | 71.57 ± 0.17 | 69.55 ± 0.36 | 81.48 ± 0.24 | 70.86 ± 0.31 | 71.50 ± 0.07 |
| $\alpha = 0.2$ | 77.98 ± 0.36 | 78.40 ± 0.22 | 78.65 ± 0.26 | 84.41 ± 0.11 | 78.76 ± 0.26 | 79.04 ± 0.01 |

Table 7: Learning with stateless clients, regarding training ResNet18 on split-CIFAR10 with $\alpha = 0.2$. All examined algorithms use FedAvg as the backbone. The details w.r.t. CFL-Regularization refer to Appendix C.1.2.

| Algorithm | FL baselines | | | CFL methods | |
|-----------|------------------|------------------|------------------|--------------------|------------------------------------|
| | FedAvg | MimeLite | FedProx | CFL-Regularization | CFL-Regularization + FedProx |
| Accuracy | 78.07 ± 0.06 | 78.47 ± 0.19 | 78.48 ± 0.05 | 79.07 ± 0.25 | 79.32 ± 0.07 |

approximation is more crucial for complicated tasks. Similarly, we demonstrate in Figure 7 (in Appendix C.1.3) that *CFL methods offer better resistance to time-evolving non-iid data* and the significance of such finding is depending on the task difficulty.

- For CFL-Regularization method, applying regularization terms on top layers works better than that on all layers. This observation matches the recent work on decoupling feature extractor and classifier (Collins et al., 2021; Chen & Chao, 2021; Luo et al., 2021): the bottom layers are more generic across tasks and can serve as a global feature extractor, while the top layers are subject to task-specific information.

We further investigate the connection between the information loss and the learning performance in Figure 3. We examine CFL methods with naive core sets, where the degree of information loss⁶ can be changed by altering the core set size from 20 to 150, with the same random seed and optimizers. Figure 3 depicts that the *performance of models is highly linked to the value of information loss: the lesser the information loss, the higher the performance*.

5.3.3 Superior Performance of CFL Methods over Other Strong FL Baselines

Alongside the comparison between CFL methods and FedAvg on various data sets (Table 5), in Table 6 we verify the efficacy of CFL methods over other strong FL baselines, on split-CIFAR10 data set. We also examine MimeLite (Karimireddy et al., 2020a), a method suggested for stateless FL scenarios. Note that we exclude the results illustration for methods like SCAFFOLD (Karimireddy et al., 2020b) and Ditto (Li et al., 2021), due to their infeasibility to be applied in our continual scenarios⁷. We also examine overlapping local data sets in Table 9 of Appendix C.1.3. Results reveal that the advancement of CFL methods is consistent with Table 6.

⁶We estimate the information loss by using $\frac{1}{tS} \sum_{i=1}^S \sum_{\tau=1}^t \|\Delta_{\tau,i}(\omega)\|$, where $\Delta_{\tau,i}(\omega)$ is defined in Equation (4), S is the number of clients chosen in each round, and t is the number of communication rounds.

⁷We also naively adapted and examined these methods, but we cannot observe significant performance gains.

5.3.4 Investigating Stateless FL Scenario

In previous numerical investigations, we examine the *stateful clients* and assume that these clients would learn and retain their client states throughout the training process. The remainder of this section will discuss learning with *stateless clients* (i.e. each client only appear once). To do this, we change the data partition strategy such that fresh data partitions are sampled on the fly for each client and communication round.

Table 7 evaluates the above-mentioned scenario. We find that *CFL-Regularization methods consistently outperform alternative FL baselines*, similar to the observations in Table 6. However, due to the nature of stateless under the privacy concern, the advancements of core set method in CFL algorithm cannot be seen in this scenario. Additionally, we discuss the applicability of different algorithms in a variety of time-evolving scenarios in Table 8 of Appendix C.1.3.

6 Conclusion and Future Work

In this paper, we formally define Continual Federated Learning (CFL) and demonstrate the necessity of saving information from previous rounds in order to improve convergence through theoretical analysis. Additionally, we find that the quality of approximation methods has a significant impact on the convergence of CFL.

We propose that designing approximation methods with reduced information loss in Federated Learning (FL) would be a valuable research direction. Additionally, exploring the potential of more advanced Continual Learning (CL) methods to enhance FL is worth investigating.

References

- Thang D Bui, Cuong V Nguyen, Siddharth Swaroop, and Richard E Turner. Partitioned variational inference: A unified framework encompassing federated and continual learning. *arXiv preprint arXiv:1811.11206*, 2018.
- Fernando E. Casado, Dylan Lema, Marcos F. Criado, Roberto Iglesias, Carlos V. Regueiro, and Senén Barro. Concept drift detection and adaptation for federated and continual learning. *CoRR*, abs/2105.13309, 2021. URL <https://arxiv.org/abs/2105.13309>.
- Francisco M Castro, Manuel J Marín-Jiménez, Nicolás Guil, Cordelia Schmid, and Karteek Alahari. End-to-end incremental learning. In *Proceedings of the European conference on computer vision (ECCV)*, pp. 233–248, 2018.
- Hong-You Chen and Wei-Lun Chao. On bridging generic and personalized federated learning. *arXiv preprint arXiv:2107.00778*, 2021.
- Liam Collins, Hamed Hassani, Aryan Mokhtari, and Sanjay Shakkottai. Exploiting shared representations for personalized federated learning. In *arXiv preprint arXiv:2102.07078*, 2021.
- Rudrajit Das, Anish Acharya, Abolfazl Hashemi, Sujay Sanghavi, Inderjit S Dhillon, and Ufuk Topcu. Faster non-convex federated learning via global and local momentum. *arXiv preprint arXiv:2012.04061*, 2020.
- Enmao Diao, Jie Ding, and Vahid Tarokh. Heteroff: Computation and communication efficient federated learning for heterogeneous clients. In *International Conference on Learning Representations*, 2021. URL <https://openreview.net/forum?id=TNkPBBYFkXg>.
- Canh T Dinh, Nguyen H Tran, and Tuan Dung Nguyen. Personalized federated learning with moreau envelopes. In *Advances in Neural Information Processing Systems*, 2020.
- Robert M French. Catastrophic forgetting in connectionist networks. *Trends in cognitive sciences*, 3(4):128–135, 1999.
- Ian J. Goodfellow, Jean Pouget-Abadie, Mehdi Mirza, Bing Xu, David Warde-Farley, Sherjil Ozair, Aaron Courville, and Yoshua Bengio. Generative adversarial networks, 2014.
- Robert Mansel Gower, Nicolas Loizou, Xun Qian, Alibek Sailanbayev, Egor Shulgin, and Peter Richtárik. Sgd: General analysis and improved rates. In *International Conference on Machine Learning*, pp. 5200–5209. PMLR, 2019.
- Farzin Haddadpour, Mohammad Mahdi Kamani, Aryan Mokhtari, and Mehrdad Mahdavi. Federated learning with compression: Unified analysis and sharp guarantees. In *International Conference on Artificial Intelligence and Statistics*, pp. 2350–2358. PMLR, 2021.
- Filip Hanzely and Peter Richtárik. Federated learning of a mixture of global and local models. *arXiv preprint arXiv:2002.05516*, 2020.
- Tzu-Ming Harry Hsu, Hang Qi, and Matthew Brown. Measuring the effects of non-identical data distribution for federated visual classification. *arXiv preprint arXiv:1909.06335*, 2019.
- Ellango Jothimurugesan, Kevin Hsieh, Jianyu Wang, Gauri Joshi, and Phillip B Gibbons. Federated learning under distributed concept drift. *arXiv preprint arXiv:2206.00799*, 2022.
- Peter Kairouz, H Brendan McMahan, Brendan Avent, Aurélien Bellet, Mehdi Bennis, Arjun Nitin Bhagoji, Kallista Bonawitz, Zachary Charles, Graham Cormode, Rachel Cummings, et al. Advances and open problems in federated learning. *arXiv preprint arXiv:1912.04977*, 2019.
- Sai Praneeth Karimireddy, Martin Jaggi, Satyen Kale, Mehryar Mohri, Sashank J Reddi, Sebastian U Stich, and Ananda Theertha Suresh. Mime: Mimicking centralized stochastic algorithms in federated learning. *arXiv preprint arXiv:2008.03606*, 2020a.
- Sai Praneeth Karimireddy, Satyen Kale, Mehryar Mohri, Sashank Reddi, Sebastian Stich, and Ananda Theertha Suresh. Scaffold: Stochastic controlled averaging for federated learning. In *International Conference on Machine Learning*, pp. 5132–5143. PMLR, 2020b.
- Ahmed Khaled, Konstantin Mishchenko, and Peter Richtárik. Tighter theory for local sgd on identical and heterogeneous data. In *International Conference on Artificial Intelligence and Statistics*, pp. 4519–4529. PMLR, 2020.
- James Kirkpatrick, Razvan Pascanu, Neil Rabinowitz, Joel Veness, Guillaume Desjardins, Andrei A Rusu, Kieran Milan, John Quan, Tiago Ramalho, Agnieszka Grabska-Barwinska, et al. Overcoming catastrophic forgetting in neural networks. *Proceedings of the national academy of sciences*, 114(13):3521–3526, 2017.
- Anastasia Koloskova, Nicolas Loizou, Sadra Boreiri, Martin Jaggi, and Sebastian Stich. A unified theory of decentralized sgd with changing topology and local updates. In *International Conference on Machine Learning*, pp. 5381–5393. PMLR, 2020.
- Tian Li, Anit Kumar Sahu, Manzil Zaheer, Maziar Sanjabi, Ameet Talwalkar, and Virginia Smith. Federated optimization in heterogeneous networks. *arXiv preprint arXiv:1812.06127*, 2018.

- Tian Li, Maziar Sanjabi, Ahmad Beirami, and Virginia Smith. Fair resource allocation in federated learning. In *8th International Conference on Learning Representations, ICLR 2020, Addis Ababa, Ethiopia, April 26-30, 2020*. OpenReview.net, 2020a. URL <https://openreview.net/forum?id=ByexELSYDr>.
- Tian Li, Shengyuan Hu, Ahmad Beirami, and Virginia Smith. Ditto: Fair and robust federated learning through personalization. In *International Conference on Machine Learning*, pp. 6357–6368. PMLR, 2021.
- Xiang Li, Kaixuan Huang, Wenhao Yang, Shusen Wang, and Zhihua Zhang. On the convergence of fedavg on non-iid data. In *International Conference on Learning Representations, 2020b*. URL <https://openreview.net/forum?id=HJxNANVtDS>.
- Zhizhong Li and Derek Hoiem. Learning without forgetting. *IEEE transactions on pattern analysis and machine intelligence*, 40(12):2935–2947, 2017.
- Tao Lin, Lingjing Kong, Sebastian U Stich, and Martin Jaggi. Ensemble distillation for robust model fusion in federated learning. In *Advances in Neural Information Processing Systems, 2020a*.
- Tao Lin, Sebastian U. Stich, Kumar Kshitij Patel, and Martin Jaggi. Don’t use large mini-batches, use local sgd. In *International Conference on Learning Representations, 2020b*. URL <https://openreview.net/forum?id=B1ey01BFPr>.
- Mi Luo, Fei Chen, Dapeng Hu, Yifan Zhang, Jian Liang, and Jiashi Feng. No fear of heterogeneity: Classifier calibration for federated learning with non-iid data. *arXiv preprint arXiv:2106.05001*, 2021.
- Davide Maltoni and Vincenzo Lomonaco. Continuous learning in single-incremental-task scenarios. *Neural Networks*, 116:56–73, 2019.
- Brendan McMahan, Eider Moore, Daniel Ramage, Seth Hampson, and Blaise Aguera y Arcas. Communication-efficient learning of deep networks from decentralized data. In *Artificial Intelligence and Statistics*, pp. 1273–1282. PMLR, 2017.
- Aritra Mitra, Rayana Jaafar, George J Pappas, and Hamed Hassani. Achieving linear convergence in federated learning under objective and systems heterogeneity. *arXiv preprint arXiv:2102.07053*, 2021.
- Mehryar Mohri, Gary Sivek, and Ananda Theertha Suresh. Agnostic federated learning. In Kamalika Chaudhuri and Ruslan Salakhutdinov (eds.), *Proceedings of the 36th International Conference on Machine Learning, ICML 2019, 9-15 June 2019, Long Beach, California, USA*, volume 97 of *Proceedings of Machine Learning Research*, pp. 4615–4625. PMLR, 2019. URL <http://proceedings.mlr.press/v97/mohri19a.html>.
- Aditya Nori, Chung-Kil Hur, Sriram Rajamani, and Selva Samuel. R2: An efficient mcmc sampler for probabilistic programs. In *Proceedings of the AAAI Conference on Artificial Intelligence*, volume 28, 2014.
- Kumar Kshitij Patel and Aymeric Dieuleveut. Communication trade-offs for synchronized distributed sgd with large step size. In *Advances in Neural Information Processing Systems, 2019*.
- Sylvestre-Alvise Rebuffi, Alexander Kolesnikov, Georg Sperl, and Christoph H Lampert. icarl: Incremental classifier and representation learning. In *Proceedings of the IEEE conference on Computer Vision and Pattern Recognition*, pp. 2001–2010, 2017.
- Sashank J. Reddi, Zachary Charles, Manzil Zaheer, Zachary Garrett, Keith Rush, Jakub Konečný, Sanjiv Kumar, and Hugh Brendan McMahan. Adaptive federated optimization. In *International Conference on Learning Representations, 2021*. URL <https://openreview.net/forum?id=LkFG31B13U5>.
- Amirhossein Reisizadeh, Farzan Farnia, Ramtin Pedarsani, and Ali Jadbabaie. Robust federated learning: The case of affine distribution shifts. In Hugo Larochelle, Marc’Aurelio Ranzato, Raia Hadsell, Maria-Florina Balcan, and Hsuan-Tien Lin (eds.), *Advances in Neural Information Processing Systems 33: Annual Conference on Neural Information Processing Systems 2020, NeurIPS 2020, December 6-12, 2020, virtual, 2020*. URL <https://proceedings.neurips.cc/paper/2020/hash/f5e536083a438cec5b64a4954abc17f1-Abstract.html>.
- Andrei A Rusu, Neil C Rabinowitz, Guillaume Desjardins, Hubert Soyer, James Kirkpatrick, Koray Kavukcuoglu, Razvan Pascanu, and Raia Hadsell. Progressive neural networks. *arXiv preprint arXiv:1606.04671*, 2016.
- Claude Sammut and Geoffrey I. Webb (eds.). *Neuro-Dynamic Programming*, pp. 716–716. Springer US, Boston, MA, 2010. ISBN 978-0-387-30164-8. doi: 10.1007/978-0-387-30164-8_588. URL https://doi.org/10.1007/978-0-387-30164-8_588.
- Neta Shoham, Tomer Avidor, Aviv Keren, Nadav Israel, Daniel Benditkis, Liron Mor-Yosef, and Itai Zeitak. Overcoming forgetting in federated learning on non-iid data. *CoRR*, abs/1910.07796, 2019. URL <http://arxiv.org/abs/1910.07796>.
- Sebastian U. Stich. Local SGD converges fast and communicates little. In *International Conference on Learning Representations, 2019*. URL <https://openreview.net/forum?id=S1g2JnRcFX>.

- Sebastian U Stich and Sai Praneeth Karimireddy. The error-feedback framework: Better rates for sgd with delayed gradients and compressed updates. *Journal of Machine Learning Research*, 21:1–36, 2020.
- Anastasiia Usmanova, François Portet, Philippe Lalanda, and German Vega. A distillation-based approach integrating continual learning and federated learning for pervasive services, 2021.
- Jianyu Wang, Qinghua Liu, Hao Liang, Gauri Joshi, and H Vincent Poor. Tackling the objective inconsistency problem in heterogeneous federated optimization. *arXiv preprint arXiv:2007.07481*, 2020.
- Blake Woodworth, Kumar Kshitij Patel, and Nathan Srebro. Minibatch vs local sgd for heterogeneous distributed learning. In *NeurIPS 2020 - Thirty-fourth Conference on Neural Information Processing Systems*, 2020a.
- Blake Woodworth, Kumar Kshitij Patel, Sebastian Stich, Zhen Dai, Brian Bullins, Brendan McMahan, Ohad Shamir, and Nathan Srebro. Is local sgd better than minibatch sgd? In *International Conference on Machine Learning*, pp. 10334–10343. PMLR, 2020b.
- Chencheng Xu, Zhiwei Hong, Minlie Huang, and Tao Jiang. Acceleration of federated learning with alleviated forgetting in local training. *arXiv preprint arXiv:2203.02645*, 2022.
- Zhewei Yao, Amir Gholami, Kurt Keutzer, and Michael W. Mahoney. Pyhessian: Neural networks through the lens of the hessian. In Xintao Wu, Chris Jermaine, Li Xiong, Xiaohua Hu, Olivera Kotevska, Siyuan Lu, Weiya Xu, Srinivas Aluru, Chengxiang Zhai, Eyhab Al-Masri, Zhiyuan Chen, and Jeff Saltz (eds.), *IEEE International Conference on Big Data, Big Data 2020, Atlanta, GA, USA, December 10-13, 2020*, pp. 581–590. IEEE, 2020. doi: 10.1109/BigData50022.2020.9378171. URL <https://doi.org/10.1109/BigData50022.2020.9378171>.
- Dong Yin, Mehrdad Farajtabar, and Ang Li. SOLA: continual learning with second-order loss approximation. *CoRR*, abs/2006.10974, 2020a. URL <https://arxiv.org/abs/2006.10974>.
- Dong Yin, Mehrdad Farajtabar, Ang Li, Nir Levine, and Alex Mott. Optimization and generalization of regularization-based continual learning: a loss approximation viewpoint. *arXiv preprint arXiv:2006.10974*, 2020b.
- Jaehong Yoon, Wonyong Jeong, Giwoong Lee, Eunho Yang, and Sung Ju Hwang. Federated continual learning with weighted inter-client transfer. In *International Conference on Machine Learning*, pp. 12073–12086. PMLR, 2021.
- Mikhail Yurochkin, Mayank Agarwal, Soumya Ghosh, Kristjan Greenewald, Nghia Hoang, and Yasaman Khazaeni. Bayesian nonparametric federated learning of neural networks. In *International Conference on Machine Learning*, pp. 7252–7261. PMLR, 2019.
- Friedemann Zenke, Ben Poole, and Surya Ganguli. Continual learning through synaptic intelligence. In *International Conference on Machine Learning*, pp. 3987–3995. PMLR, 2017.
- Guodong Zhang, Lala Li, Zachary Nado, James Martens, Sushant Sachdeva, George E Dahl, Christopher J Shallue, and Roger Grosse. Which algorithmic choices matter at which batch sizes? insights from a noisy quadratic model. In *Advances in Neural Information Processing Systems*, 2019.
- Chen Zhu, Zheng Xu, Mingqing Chen, Jakub Konečný, Andrew Hard, and Tom Goldstein. Diurnal or nocturnal? federated learning of multi-branch networks from periodically shifting distributions. In *International Conference on Learning Representations*, 2021.
- Martin Zinkevich, Markus Weimer, Alexander J Smola, and Lihong Li. Parallelized stochastic gradient descent. In *NIPS*, volume 4, pp. 4. Citeseer, 2010.

Contents of Appendix

| | | |
|----------|--|-----------|
| A | Techniques | 18 |
| B | Convergence Rate of CFL | 18 |
| B.1 | Bound of Gradient Noise | 19 |
| B.2 | Bounded Gradient Noise of CFL | 19 |
| B.3 | Bounded Approximation Error | 19 |
| B.4 | Proof of Theorem 4.1 | 20 |
| B.4.1 | Preliminaries | 20 |
| B.4.2 | One Step Progress | 20 |
| B.4.3 | Weights of rounds. | 23 |
| B.4.4 | Convergence results | 23 |
| B.5 | Proof of Convergence Rate for Non-convex Setting | 24 |
| B.6 | Theoretical Results | 26 |
| B.7 | Convergence Rate of CFL under Correlated Time Drifts | 27 |
| B.8 | Proof of Theorem 7 | 28 |
| C | Experiment details | 30 |
| C.1 | Realistic Data Sets | 30 |
| C.1.1 | Setup | 30 |
| C.1.2 | Approximation Methods | 30 |
| C.1.3 | Additional Experiments | 31 |
| C.2 | Algorithms | 32 |

A Techniques

Here we show some technical lemmas which are helpful in the theoretical proof.

Lemma A.1 (Linear convergence rate (Karimireddy et al., 2020b, Lemma 1)). *For every non-negative sequence $\{d_{r-1}\}_{r \geq 1}$, and any parameter $\mu > 0$, $T \geq \frac{1}{2\eta_{max}\mu}$, there exists a constant step-size $\eta \leq \eta_{max}$ and weights $\omega_t = (1 - \mu\eta)^{1-t}$ such that for $W_T = \sum_{t=1}^{T+1} \omega_t$*

$$\Phi_T = \frac{1}{W_T} \sum_{t=1}^{T+1} \left(\frac{\omega_{t-1}}{\eta} (1 - \mu\eta) d_{t-1} - \frac{\omega_t}{\eta} d_t \right) = \mathcal{O}(\mu d_0 \exp(-\mu\eta_{max}T)).$$

Lemma A.2 (Sub-linear convergence rate (Karimireddy et al., 2020b, Lemma 2)). *For every non-negative sequence $\{d_{r-1}\}_{r \geq 1}$ and any parameters $\eta_{max} > 0$, $c_1 \geq 0$, $c_2 \geq 0$, $T \geq 0$, there exists a constant step-size $\eta \leq \eta_{max}$ such that*

$$\Phi_T = \frac{1}{T+1} \sum_{t=1}^{T+1} \left(\frac{d_{t-1}}{\eta} - \frac{d_t}{\eta} + c_1\eta + c_2\eta^2 \right) \leq \frac{d_0}{\eta_{max}(T+1)} + \frac{2\sqrt{c_1 d_0}}{\sqrt{T+1}} + 2 \left(\frac{d_0}{T+1} \right)^{\frac{2}{3}} c_2^{\frac{1}{3}}.$$

Lemma A.3 (Relaxed triangle inequality (Karimireddy et al., 2020b, Lemma 3)). *Let $\{\mathbf{v}_1, \dots, \mathbf{v}_\tau\}$ be τ vectors in \mathcal{R}^d . Then the following is true:*

$$\left\| \frac{1}{\tau} \sum_{i=1}^{\tau} \mathbf{v}_i \right\|^2 \leq \frac{1}{\tau} \sum_{i=1}^{\tau} \|\mathbf{v}_i\|^2.$$

Lemma A.4 (Separating mean and variance (Stich & Karimireddy, 2020, Lemma 14)). *Let $\Xi_1, \Xi_2, \dots, \Xi_\tau$ be τ random variables in \mathcal{R}^d which are not necessarily independent. First suppose that their mean is $E[\Xi_i] = \xi_i$, and variance is bounded as $\mathbb{E}\|\Xi_i - \xi_i\|^2 \leq M\|\xi_i\|^2 + \sigma^2$, then the following holds*

$$\mathbb{E}\left\| \sum_{i=1}^{\tau} \Xi_i \right\|^2 \leq (\tau + M) \sum_{i=1}^{\tau} \|\xi_i\|^2 + \tau\sigma^2.$$

Lemma A.5 (Perturbed strongly convexity (Karimireddy et al., 2020b, Lemma 5)). *The following holds for any L -smooth and μ -strongly convex function h , and any $\mathbf{x}, \mathbf{y}, \mathbf{z}$ in the domain of h*

$$\langle \nabla h(\mathbf{x}), \mathbf{z} - \mathbf{y} \rangle \geq h(\mathbf{z}) - h(\mathbf{y}) + \frac{\mu}{4} \|\mathbf{y} - \mathbf{z}\|^2 - L \|\mathbf{z} - \mathbf{x}\|^2.$$

Lemma A.6. *Define $S = \sum_{t=1}^T \frac{p_t}{t}$ where $\sum_{t=1}^T p_t = 1$, and $p_t \leq p_{t+1}$ then $S \leq \frac{1}{T} \sum_{t=1}^T \frac{1}{t} = \mathcal{O}\left(\frac{\ln T}{T}\right)$.*

B Convergence Rate of CFL

In this section, we will provide the theoretical proof of the convergence rates of CFL and FedAvg in time-varying scenarios under Assumptions 1–4). We will prove Theorems 4.1, 4.4, 4.7, and 4.9. Before proceeding with the proof, we will introduce some useful lemmas.

B.1 Bound of Gradient Noise

Lemma B.1 (Bound of Gradient Noise). *Suppose $f_i(\boldsymbol{\omega})$ is the local objective function, and $f(\boldsymbol{\omega}) = \mathbb{E}[f_i(\boldsymbol{\omega})]$ is the global objective function. Define $\nabla f(\boldsymbol{\omega}) = \nabla f_i(\boldsymbol{\omega}) + \boldsymbol{\varsigma}_i$, $\mathbb{E}[\boldsymbol{\varsigma}_i] = 0$, and assume $\mathbb{E}[\|\boldsymbol{\varsigma}_i\|^2 | \boldsymbol{\omega}] \leq A^2 \mathbb{E}[\|\nabla f(\boldsymbol{\omega})\|^2] + B^2$, we have*

$$\mathbb{E}[\|\nabla f_i(\boldsymbol{\omega})\|^2] \leq (A^2 + 1)\mathbb{E}[\|\nabla f(\boldsymbol{\omega})\|^2] + B^2.$$

Proof.

$$\begin{aligned} \mathbb{E}[\|\nabla f_i(\boldsymbol{\omega})\|^2] &= \mathbb{E}[\|\nabla f(\boldsymbol{\omega}) + \boldsymbol{\varsigma}_i\|^2] = \mathbb{E}[\|\nabla f(\boldsymbol{\omega})\|^2] + \mathbb{E}[\|\boldsymbol{\varsigma}_i\|^2], \\ &\leq (A + 1)\mathbb{E}[\|\nabla f(\boldsymbol{\omega})\|^2] + B. \end{aligned}$$

□

B.2 Bounded Gradient Noise of CFL

Lemma B.2 (Bounded Gradient Noise of CFL). *For Formulation (2), consider CFL and FedAvg, we can bound the gradient drift as*

(1) *FedAvg only optimize current local objective functions, thus*

$$\mathbb{E}\|\nabla f_{t,i}(\boldsymbol{\omega})\|^2 \leq (1 + A^2 + B^2)\mathbb{E}\|\nabla f(\boldsymbol{\omega})\|^2 + G^2 + D^2.$$

(2) *For CFL, in general (same clients can appear in different rounds), we have*

$$\mathbb{E}\left\|\sum_{\tau=1}^t p_{\tau,i} \nabla f_{\tau,i}(\boldsymbol{\omega})\right\|^2 \leq (1 + B^2 + A^2 \sum_{\tau=1}^t p_{\tau,i}^2) \mathbb{E}\|\nabla f(\boldsymbol{\omega})\|^2 + G^2 + D^2 \sum_{\tau=1}^t p_{\tau,i}^2.$$

(3) *For CFL, when clients only participate in training once ($\boldsymbol{\delta}_{t,i}$ are independent for all t and i), we have*

$$\mathbb{E}\left\|\sum_{\tau=1}^t p_{\tau,i} \nabla f_{\tau,i}(\boldsymbol{\omega})\right\|^2 \leq (1 + (B^2 + A^2) \sum_{\tau=1}^t p_{\tau,i}^2) \mathbb{E}\|\nabla f(\boldsymbol{\omega})\|^2 + (G^2 + D^2) \sum_{\tau=1}^t p_{\tau,i}^2.$$

Proof. Using Assumption 3, together with the fact that $\nabla f_{t,i}(\boldsymbol{\omega}) = \nabla f(\boldsymbol{\omega}) + \boldsymbol{\delta}_{t,i} + \boldsymbol{\xi}_{t,i}$ (Here to simplify the notation, we use $\{t, i\}$ pair to denote the client participate in training on round t and number i), we have

$$\begin{aligned} \mathbb{E}\|\nabla f_{t,i}(\boldsymbol{\omega})\|^2 &= \mathbb{E}\|\nabla f(\boldsymbol{\omega}) + \boldsymbol{\delta}_{t,i} + \boldsymbol{\xi}_{t,i}\|^2 = \mathbb{E}\|\nabla f(\boldsymbol{\omega})\|^2 + \mathbb{E}\|\boldsymbol{\delta}_{t,i}\|^2 + \mathbb{E}\|\boldsymbol{\xi}_{t,i}\|^2 \\ &\leq (1 + A^2 + B^2)\mathbb{E}\|\nabla f(\boldsymbol{\omega})\|^2 + G^2 + D^2. \end{aligned}$$

The second inequality is based on the independence of noise, and directly use Assumption 3 we get the last inequality. Similarly, we have

$$\begin{aligned} \mathbb{E}\left\|\sum_{\tau=1}^t p_{\tau,i} \nabla f_{\tau,i}(\boldsymbol{\omega})\right\|^2 &= \mathbb{E}\left\|\sum_{\tau=1}^t p_{\tau,i} (\nabla f_{\tau,i}(\boldsymbol{\omega}) + \boldsymbol{\delta}_{\tau,i} + \boldsymbol{\xi}_{\tau,i})\right\|^2 \\ &= \mathbb{E}\|\nabla f(\boldsymbol{\omega})\|^2 + \mathbb{E}\|\boldsymbol{\delta}_i\|^2 + \mathbb{E}\left\|\sum_{\tau=1}^t p_{\tau,i} \boldsymbol{\xi}_{\tau,i}\right\|^2 \\ &\leq (1 + B^2 + A^2 \sum_{\tau=1}^t p_{\tau,i}^2) \mathbb{E}\|\nabla f(\boldsymbol{\omega})\|^2 + G^2 + D^2 \sum_{\tau=1}^t p_{\tau,i}^2. \end{aligned}$$

For the last inequality, when $\boldsymbol{\delta}_{t_1,i}$ and $\boldsymbol{\delta}_{t_2,i}$ are independent for all t_1, t_2

$$\begin{aligned} \mathbb{E}\left\|\sum_{\tau=1}^t p_{\tau,i} \nabla f_{\tau,i}(\boldsymbol{\omega})\right\|^2 &= \mathbb{E}\left\|\sum_{\tau=1}^t p_{\tau,i} (\nabla f_{\tau,i}(\boldsymbol{\omega}) + \boldsymbol{\delta}_{\tau,i} + \boldsymbol{\xi}_{\tau,i})\right\|^2 \\ &= \mathbb{E}\|\nabla f(\boldsymbol{\omega})\|^2 + \mathbb{E}\left\|\sum_{\tau=1}^t p_{\tau,i} \boldsymbol{\delta}_{\tau,i}\right\|^2 + \mathbb{E}\left\|\sum_{\tau=1}^t p_{\tau,i} \boldsymbol{\xi}_{\tau,i}\right\|^2 \\ &\leq (1 + (A^2 + B^2) \sum_{\tau=1}^t p_{\tau,i}^2) \mathbb{E}\|\nabla f(\boldsymbol{\omega})\|^2 + (G^2 + D^2) \sum_{\tau=1}^t p_{\tau,i}^2. \end{aligned}$$

□

B.3 Bounded Approximation Error

Lemma B.3 (Bounded Approximation Error). *For $\Delta_{t,i}(\boldsymbol{\omega}) = \nabla f_{t,i}(\boldsymbol{\omega}) - \nabla \tilde{f}_{t,i}(\boldsymbol{\omega})$ (c.f. Definition 4), if we assume that $\|\nabla^2 f_{t,i}(\boldsymbol{\omega}_1) - \nabla^2 f_{t,i}(\boldsymbol{\omega}_2)\| \leq \epsilon$, when use Taylor Extension,*

$$\nabla \tilde{f}_{t,i}(\boldsymbol{\omega}) = \nabla f_{t,i}(\boldsymbol{\omega}_t) + \nabla^2 f_{t,i}(\boldsymbol{\omega}_t)(\boldsymbol{\omega} - \boldsymbol{\omega}_t),$$

we have

$$\|\Delta_{t,i}(\boldsymbol{\omega})\| \leq \epsilon \|\boldsymbol{\omega} - \hat{\boldsymbol{\omega}}_{t,i}\|.$$

Algorithm 2 CFL Framework

Require: initial weights ω_0 , global learning rate η_g , local learning rate η_l

```

1: for round  $t = 1, \dots, T$  do
2:   communicate  $\omega_t$  to the chosen clients.
3:   for client  $i \in \mathcal{S}_t$  in parallel do
4:     initialize local model  $\omega_{t,i,0} = \omega_t$ .
5:     for  $k = 1, \dots, K$  do
6:        $\tilde{g}_{t,i,k}(\omega_{t,i,k-1}) = \left( p_{t,i} \nabla f_{t,i}(\omega_{t,i,k-1}) + \sum_{\tau=1}^{t-1} p_{\tau,i} \nabla \tilde{f}_{\tau,i}(\omega_{t,i,k-1}) \right) + \nu_{t,i,k}$ .
7:        $\omega_{t,i,k} \leftarrow \omega_{t,i,k-1} - \eta_l \tilde{g}_{t,i,k}(\omega_{t,i,k-1})$ .
8:       communicate  $\Delta\omega_{t,i} \leftarrow \omega_{t,i,K} - \omega_t$ .
9:      $\Delta\omega_t \leftarrow \frac{\eta_g}{S} \sum_{i \in \mathcal{S}_t} \Delta\omega_{t,i}$ .
10:   $\omega_{t+1} \leftarrow \omega_t + \Delta\omega_t$ .
  
```

Proof.

$$\begin{aligned}
\|\Delta_{t,i}(\omega)\| &= \left\| \nabla f_{t,i}(\omega) - \nabla \tilde{f}_{t,i}(\omega) \right\| = \left\| \nabla f_{t,i}(\omega) - \nabla f_{t,i}(\omega_{t,i,K}) - \mathbf{H}_{tjK}(\omega - \omega_{t,i,K}) \right\|, \\
&= \left\| \nabla^2 f_{t,i}(\omega_{\xi,t})(\omega - \omega_{t,i,K}) - \mathbf{H}_{tjK}(\omega - \omega_{t,i,K}) \right\| = \left\| (\nabla^2 f_{t,i}(\omega_{\xi,t}) - \mathbf{H}_{tjK})(\omega - \omega_{t,i,K}) \right\|, \\
&\leq \epsilon \|\omega - \omega_{t,i,K}\|.
\end{aligned}$$

The first two equations come from the mean value theorem which says for continuous function f in closed intervals $[a, b]$ and differentiable on open interval (a, b) , there exists a point $c \subseteq (a, b)$ such that $f'(c) = \frac{f(b)-f(a)}{b-a}$. \square

B.4 Proof of Theorem 4.1

In this section we will give the complete proof of convergence rate of Algorithm 2 when the local objective functions are convex.

B.4.1 Preliminaries

The local objective function of round t on client i is

$$\tilde{f}_{t,i}(\omega) = (p_{t,i} f_{t,i}(\omega) + \sum_{\tau=1}^{t-1} p_{\tau,i} \tilde{f}_{\tau,i}(\omega)).$$

Without loss of generality, assume $\sum_{\tau=1}^t p_{\tau,i} = 1$. Then follow the steps in Algorithm 2, we have

$$\nabla \tilde{f}_{t,i}(\omega) = p_{t,i} \nabla f_{t,i}(\omega) + \sum_{\tau=1}^{t-1} p_{\tau,i} \nabla \tilde{f}_{\tau,i}(\omega).$$

Then the noisy gradient in mini-batch SGD can be described as

$$\bar{g}_{t,i,k}(\omega_{t,i,k-1}) = \nabla \tilde{f}_{t,i}(\omega_{t,i,k-1}) + \nu_{t,i,k}.$$

Then follow the steps in Algorithm 2, we have

$$\begin{aligned}
\Delta\omega_t &= \frac{-\eta_l \eta_g}{N} \sum_{i=1}^N \sum_{k=1}^K \bar{g}_{t,i}(\omega_{t,i,k-1}), \\
E[\Delta\omega_t] &= \frac{-\eta_l \eta_g}{N} \sum_{i=1}^N \sum_{k=1}^K \nabla \tilde{f}_{t,i}(\omega_{t,i,k-1}).
\end{aligned}$$

Then let $\eta = K\eta_l\eta_g$, we have

$$\Delta\omega_t = \frac{-\eta}{NK} \sum_{i=1}^N \sum_{k=1}^K \bar{g}_{t,i}(\omega_{t,i,k-1}), \quad (8)$$

$$E[\Delta\omega_t] = \frac{-\eta}{NK} \sum_{i=1}^N \sum_{k=1}^K \nabla \tilde{f}_{t,i}(\omega_{t,i,k-1}). \quad (9)$$

B.4.2 One Step Progress

Optimizing Algorithm 2 for one step, we can find that

$$\mathbb{E}\|\omega_t + \Delta\omega_t - \omega^*\|^2 = \|\omega_t - \omega^*\|^2 - \underbrace{2E\langle \omega_t - \omega^*, \Delta\omega_t \rangle}_{A_1} + \underbrace{\mathbb{E}\|\Delta\omega_t\|^2}_{A_2}. \quad (10)$$

Firstly we consider A_1 part in Equation (10)

$$\begin{aligned}
& -2E\langle \omega_t - \omega^*, \Delta \omega_t \rangle = \frac{2\eta}{NK} \sum_{i=1}^N \sum_{k=1}^K \langle \nabla \bar{f}_{t,i}(\omega_{t,i,k-1}), \omega^* - \omega_t \rangle, \\
& = \frac{2\eta}{NK} \sum_{i=1}^N \sum_{k=1}^K \langle p_{t,i} \nabla f_{t,i}(\omega_{t,i,k}) + \sum_{\tau=1}^{t-1} p_{\tau,i} \nabla \bar{f}_{\tau,i}(\omega_{t,i,k}), \omega^* - \omega_t \rangle, \\
& = \frac{2\eta}{NK} \sum_{i=1}^N \sum_{k=1}^K \sum_{\tau=1}^t \langle p_{\tau,i} \nabla f_{\tau,i}(\omega_{t,i,k}), \omega^* - \omega_t \rangle - \frac{2\eta}{NK} \sum_{i=1}^N \sum_{k=1}^K \sum_{\tau=1}^{t-1} p_{\tau,i} \langle \Delta_{\tau,i}(\omega_{t,i,k}), \omega^* - \omega_t \rangle, \\
& \leq \frac{2\eta}{NK} \sum_{i=1}^N \sum_{k=1}^K \sum_{\tau=1}^t p_{\tau,i} \langle \nabla f_{\tau,i}(\omega_{t,i,k}), \omega^* - \omega_t \rangle + \frac{2\eta}{N} \sum_{i=1}^N \sum_{\tau=1}^{t-1} p_{\tau,i} R \|\omega^* - \omega_t\|. \tag{11}
\end{aligned}$$

We use Inequality (9) to obtain the first inequality, and Assumption 4 and Cauchy–Schwarz Inequality for the last inequality. Then for the first term of Inequality (11), by applying Lemma A.5, we can conclude that

$$\langle \nabla f_{\tau,i}(\omega_{t,i,k-1}), \omega^* - \omega_t \rangle \leq f_{\tau,i}(\omega^*) - f_{\tau,i}(\omega_t) - \frac{\mu}{4} \|\omega_t - \omega^*\|^2 + L \|\omega_{t,i,k-1} - \omega_t\|. \tag{12}$$

Combine Inequality (11) and Inequality (12), we have

$$\begin{aligned}
& -2E\langle \omega_t - \omega^*, \Delta \omega_t \rangle \\
& \leq -2\eta(f_t(\omega_t) - f_t(\omega^*) + \frac{\mu}{4} \|\omega_t - \omega^*\|^2) + \frac{2\eta L}{NK} \sum_{i=1}^N \sum_{k=1}^K \|\omega_{t,i,k-1} - \omega_t\|^2 \\
& \quad + 2\eta \sum_{\tau=1}^{t-1} p_{\tau,i} R \|\omega^* - \omega_t\|. \tag{13}
\end{aligned}$$

Secondly, we are willing to deal with A_2 in Equation (10). Define $c_{p_B,i} = 1 + B^2 + A^2(\sum_{\tau=1}^t p_{\tau,i}^2)$, $c_{p_G,i} = G^2 + D^2(\sum_{\tau=1}^t p_{\tau,i}^2)$, $c_{p_B} = \frac{1}{N} \sum_{i=1}^N c_{p_B,i}$, and $c_{p_G} = \frac{1}{N} \sum_{i=1}^N c_{p_G,i}$ we have

$$\begin{aligned}
\mathbb{E}\|\Delta \omega_t\|^2 & = \frac{\eta^2}{N^2 K^2} \mathbb{E} \left\| \sum_{i=1}^N \sum_{k=1}^K \left(p_{t,i} \nabla f_{t,i}(\omega_{t,i,k-1}) + \sum_{\tau=1}^{t-1} p_{\tau,i} \nabla \bar{f}_{\tau,i}(\omega_{t,i,k-1}) + \nu_{t,i,k} \right) \right\|^2, \\
& = \frac{\eta^2}{N^2 K^2} \mathbb{E} \left\| \sum_{i=1}^N \sum_{k=1}^K \left(\sum_{\tau=1}^t p_{\tau,i} \nabla f_{\tau,i}(\omega_{t,i,k-1}) - \sum_{\tau=1}^{t-1} p_{\tau,i} \Delta_{\tau,i}(\omega_{t,i,k-1}) + \nu_{t,i,k} \right) \right\|^2, \\
& \stackrel{\text{Lem A.4}}{\leq} \frac{\eta^2}{NK} \sum_{i=1}^N \sum_{k=1}^K \mathbb{E} \left\| \sum_{\tau=1}^t p_{\tau,i} \nabla f_{\tau,i}(\omega_{t,i,k-1}) - \sum_{\tau=1}^{t-1} p_{\tau,i} \Delta_{\tau,i}(\omega_{t,i,k-1}) \right\|^2 + \frac{\eta^2 \sigma^2}{NK}, \\
& \stackrel{\text{Lem A.3}}{\leq} \frac{2\eta^2}{NK} \sum_{i=1}^N \sum_{k=1}^K \left(\mathbb{E} \left\| \sum_{\tau=1}^t p_{\tau,i} \nabla f_{\tau,i}(\omega_{t,i,k-1}) \right\|^2 + \mathbb{E} \left\| \sum_{\tau=1}^{t-1} p_{\tau,i} \Delta_{\tau,i}(\omega_{t,i,k-1}) \right\|^2 \right) + \frac{\eta^2 \sigma^2}{NK}, \tag{14} \\
& \stackrel{\text{Lem B.2}}{\leq} \frac{2\eta^2}{NK} \sum_{i=1}^N \sum_{k=1}^K \left((1 + B^2 + A^2(\sum_{\tau=1}^t p_{\tau,i}^2)) \mathbb{E} \|\nabla f(\omega_{t,i,k-1})\|^2 + (G^2 + D^2(\sum_{\tau=1}^t p_{\tau,i}^2)) \right) \\
& \quad + \frac{2\eta^2}{N} \sum_{i=1}^N (\sum_{\tau=1}^{t-1} p_{\tau,i})^2 R^2 + \frac{\eta^2 \sigma^2}{NK}, \\
& \stackrel{\text{Lem A.3}}{\leq} \frac{4\eta^2}{NK} \sum_{i=1}^N \sum_{k=1}^K c_{p_B,i} \left(\mathbb{E} \|\nabla f(\omega_{t,i,k-1}) - \nabla f(\omega_t)\|^2 + \mathbb{E} \|\nabla f(\omega_t)\|^2 \right) + 2\eta^2 c_{p_G} \\
& \quad + \frac{2\eta^2}{N} \sum_{i=1}^N (\sum_{\tau=1}^{t-1} p_{\tau,i})^2 R^2 + \frac{\eta^2 \sigma^2}{NK}, \\
& \stackrel{\text{Ass 1}}{\leq} 16\eta^2 L c_{p_B} (f(\omega_t) - f(\omega^*)) + \frac{8\eta^2 L^2}{NK} \sum_{i=1}^N \sum_{k=1}^K c_{p_B,i} \mathbb{E} \|\omega_{t,i,k-1} - \omega_t\|^2 + 2\eta^2 c_{p_G} \\
& \quad + \frac{2\eta^2}{N} \sum_{i=1}^N (\sum_{\tau=1}^{t-1} p_{\tau,i})^2 R^2 + \frac{\eta^2 \sigma^2}{NK}. \tag{15}
\end{aligned}$$

We now turn our attention to solving $\mathbb{E}\|\omega_{t,i,k-1} - \omega_t\|^2$. By examining Inequalities (13) and (15), we can see that this is the remaining task. We can write this expectation as follows

$$\mathbb{E}\|\omega_{t,i,k} - \omega_t\|^2 = \eta_t^2 \mathbb{E} \left\| \sum_{\tau=1}^k \bar{g}_{t,i}(\omega_{t,i,\tau-1}) \right\|^2, \tag{16}$$

$$\stackrel{\text{Lem A.4}}{\leq} k\eta_t^2 \sum_{\tau=1}^k \mathbb{E} \|\nabla \bar{f}_{t,i}(\omega_{t,i,\tau-1})\|^2 + k\eta_t^2 \sigma^2. \tag{17}$$

We utilize Lemma A.4 to derive Inequality (17). The remaining challenge in this inequality is to bound $\mathbb{E}\|\nabla \bar{f}_{t,i}(\omega)\|^2$. To address this, we consider that

$$\begin{aligned}
\mathbb{E}\|\nabla \bar{f}_{t,i}(\omega)\|^2 & = \mathbb{E} \left\| p_{t,i} \nabla f_{t,i}(\omega) + \sum_{\tau=1}^{t-1} p_{\tau,i} \nabla \bar{f}_{\tau,i}(\omega) \right\|^2, = \mathbb{E} \left\| \sum_{\tau=1}^t p_{\tau,i} \nabla f_{\tau,i}(\omega) - \sum_{\tau=1}^{t-1} p_{\tau,i} \Delta_{\tau,i}(\omega) \right\|^2, \\
& \stackrel{\text{Lem A.3}}{\leq} 2\mathbb{E} \left\| \sum_{\tau=1}^t p_{\tau,i} \nabla f_{\tau,i}(\omega) \right\|^2 + 2\mathbb{E} \left\| \sum_{\tau=1}^{t-1} p_{\tau,i} \Delta_{\tau,i}(\omega) \right\|^2, \\
& \stackrel{\text{Lem B.2}}{\leq} 2c_{p_B,i} \mathbb{E} \|\nabla f(\omega)\|^2 + 2c_{p_G,i} + 2(\sum_{\tau=1}^{t-1} p_{\tau,i})^2 R^2, \\
& \stackrel{\text{Ass 1}}{\leq} 4L^2 c_{p_B,i} \mathbb{E} \|\omega - \omega_t\|^2 + 8L c_{p_B,i} (f(\omega_t) - f(\omega^*)) + 2c_{p_G,i} + 2(\sum_{\tau=1}^{t-1} p_{\tau,i})^2 R^2. \tag{18}
\end{aligned}$$

Combine Inequalities (17) and (18) we get,

$$\begin{aligned} \mathbb{E}\|\omega_{t,i,k} - \omega_t\|^2 &\leq 4k^2\eta_l^2 L^2 c_{p_B,i} \mathbb{E}\|\omega_{t,i,k-1} - \omega_t\|^2 + 8k^2\eta_l^2 L c_{p_B,i} (f(\omega_t) - f(\omega^*)) + 2k^2\eta_l^2 c_{p_G,i} \\ &+ 2k^2\eta_l^2 (\sum_{\tau=1}^{t-1} p_{\tau,i})^2 R^2 + k\eta_l^2 \sigma^2. \end{aligned} \quad (19)$$

By combining Inequalities (17) and (19) iteratively, we obtain the following result

$$\begin{aligned} \mathbb{E}\|\omega_{t,i,k} - \omega_t\|^2 &\leq \sum_{\tau=0}^{k-1} (8K^2\eta_l^2 L c_{p_B,i} (f(\omega_t) - f(\omega^*)) \\ &+ 2K^2\eta_l^2 c_{p_G,i} + 2K^2\eta_l^2 (\sum_{\tau=1}^{t-1} p_{\tau,i})^2 R^2 + K\eta_l^2 \sigma^2) (4K^2\eta_l^2 L^2 c_{p_B,i})^\tau, \\ &\leq \frac{8K^2\eta_l^2 L c_{p_B,i} (f(\omega_t) - f(\omega^*)) + 2K^2\eta_l^2 c_{p_G,i} + 2K^2\eta_l^2 (\sum_{\tau=1}^{t-1} p_{\tau,i})^2 R^2 + K\eta_l^2 \sigma^2}{1 - 4K^2\eta_l^2 L^2 c_{p_B,i}}. \end{aligned} \quad (20)$$

Combine the Inequalities (10), (13), (15), and (20), we get

$$\begin{aligned} &\mathbb{E}\|\omega_t + \Delta\omega_t - \omega^*\|^2, \\ &\leq (1 - \frac{\mu\eta}{2}) \mathbb{E}\|\omega_t - \omega^*\|^2 \\ &+ (-2\eta + 16\eta^2 L c_{p_B} + \frac{1}{N} \sum_{i=1}^N \frac{16K^2\eta_l^2 L c_{p_B,i} (1+4\eta L c_{p_B,i})}{1-4K^2\eta_l^2 L^2 c_{p_B,i}}) (f(\omega_t) - f^*) + 2\eta^2 c_{p_G} \\ &+ \frac{\eta^2 \sigma^2}{NK} + \frac{1}{N} \sum_{i=1}^N \left(2\eta^2 (\sum_{\tau=1}^{t-1} p_{\tau,i})^2 + \frac{4K^2\eta_l^2 L (\sum_{\tau=1}^{t-1} p_{\tau,i})^2 (1+4\eta L c_{p_B,i})}{1-4K^2\eta_l^2 L^2 c_{p_B,i}} \right) R^2 \\ &+ \frac{1}{N} \sum_{i=1}^N \frac{2K\eta_l^2 L (2K c_{p_G,i} + \sigma^2) (1+4\eta L c_{p_B,i})}{1-4K^2\eta_l^2 L^2 c_{p_B,i}} + \frac{2\eta}{N} \sum_{i=1}^N \sum_{\tau=1}^{t-1} p_{\tau,i} R \|\omega_t - \omega^*\|. \end{aligned} \quad (21)$$

To promise convergence, we must have

$$-2\eta + 16\eta^2 L c_{p_B} + \frac{1}{N} \sum_{i=1}^N \frac{16K^2\eta_l^2 L^2 c_{p_B,i} (1+4\eta L c_{p_B,i})}{1-4K^2\eta_l^2 L^2 c_{p_B,i}} \leq 0. \quad (22)$$

Using the fact that $\eta = K\eta_l\eta_g$, we can solve Inequality (22) and determine that if η satisfies the condition

$$\eta \leq \frac{\sqrt{3\eta_g^2 + 4c_{p_B,i}\eta_g^4} - \sqrt{4c_{p_B,i}\eta_g^4}}{6L\sqrt{c_{p_B,i}}},$$

for any $c_{p_B,i}$, convergence is guaranteed. Defining \hat{c}_{p_B} as the largest $c_{p_B,i}$, we can further simplify this condition to

$$\eta \leq \frac{\sqrt{3\eta_g^2 + 4\hat{c}_{p_B}\eta_g^4} - \sqrt{4\hat{c}_{p_B}\eta_g^4}}{12L\sqrt{\hat{c}_{p_B}}}.$$

This leads to the inequality

$$1 - 4K^2\eta_l^2 L^2 c_{p_B,i} \geq \frac{33 - 8\eta_g^2 \hat{c}_{p_B} + 4\sqrt{3\eta_g^2 \hat{c}_{p_B} + 4\eta_g^4 \hat{c}_{p_B}^2}}{36},$$

and therefore

$$\frac{1+4\eta L c_{p_B,i}}{1-4K^2\eta_l^2 L^2 c_{p_B,i}} \leq \frac{1}{12} - \frac{7}{33 + \sqrt{3\eta_g^2 \hat{c}_{p_B} + 4\eta_g^4 \hat{c}_{p_B}^2} - 2\eta_g^2 \hat{c}_{p_B}} \leq \frac{1}{12}.$$

Let $c_{R,i} = (\sum_{\tau=1}^{t-1} p_{\tau,i})^2 R^2$ and $c_R = \frac{1}{N} \sum_{i=1}^N c_{R,i}$. We assume $c_1 = 2c_{p_G} + \frac{\sigma^2}{NK} + 2c_R$, $c_2 = \frac{L c_{p_G}}{3\eta_g^2} + \frac{L\sigma^2}{6\eta_g^2 K} + \frac{L c_R}{3\eta_g^2}$, and $c_3 = \frac{2}{N} \sum_{i=1}^N \sum_{\tau=1}^{t-1} p_{\tau,i} R$. Thus, Inequality (21) can be rewritten as

$$\mathbb{E}\|\omega_t + \Delta\omega_t - \omega^*\|^2 \leq (1 - \frac{\mu\eta}{2}) \mathbb{E}\|\omega_t - \omega^*\|^2 - \eta (f(\omega_t) - f^*) + c_1\eta^2 + c_2\eta^3 + c_3\eta \|\omega_t - \omega^*\|.$$

Move $f(\omega_t) - f^*$ to the left side, we get

$$f(\omega_t) - f(\omega^*) \leq \frac{1}{\eta} (1 - \frac{\mu\eta}{2}) \mathbb{E}\|\omega_t - \omega^*\|^2 - \frac{1}{\eta} \mathbb{E}\|\omega_{t+1} - \omega^*\|^2 + c_1\eta + c_2\eta^2 + \varphi_t. \quad (23)$$

Here φ_t is a constant bounded by $c_3 \|\omega_0 - \omega^*\|$. Because of φ_t , the model cannot converge to an arbitrary ϵ ; instead, it can only converge to the neighborhood of $\epsilon + \varphi$, where φ is the weighted sum of the sequence φ_t . The following parts give the convergence rates when models converge to $\epsilon + \varphi$ for convenience.

B.4.3 Weights of rounds.

We can carefully tune the $p_{\tau,i}$ to minimize the noise while speeding up the convergence. Here we give the lemma of the best choice of $p_{\tau,i}$.

Lemma B.4. *On round t , when setting $p_{\tau,i} = \frac{D^2}{tD^2+(t-1)R^2}$ for any $\tau < t$, and $p_{t,i} = \frac{(t-1)R^2+D^2}{tD^2+(t-1)R^2}$, we can minimize c_1 and c_2 to get best convergence, where $c_1 = 2c_{p_G} + \frac{\sigma^2}{NK} + 2c_R$, and $c_2 = \frac{Lc_{p_G}}{3\eta_g^2} + \frac{L\sigma^2}{6\eta_g^2K} + \frac{Lc_R}{3\eta_g^2}$.*

Proof. Minimizing c_1 and c_2 is equal to minimize $c_{p_G} + c_R$, that is

$$\min_p \frac{1}{N} \sum_{i=1}^N (1 - p_{t,i})^2 R^2 + G^2 + D^2 \left(\sum_{\tau=1}^t p_{\tau,i}^2 \right), \text{ s.t. } \sum_{\tau=1}^t p_{\tau,i} = 1, \forall i = 1, \dots, N.$$

Solving above optimization problem, we get the results. \square

Using lemma B.4, we have $\min\{c_{p_G} + c_R\} = G^2 + D^2 \left(\frac{D^2+(t-1)R^2}{tD^2+(t-1)R^2} \right)$. Notice that the value of c_1 , c_2 , and c_3 are changing over t . We use c_1^t , c_2^t , and c_3^t to represent c_1 , c_2 , and c_3 on round t .

B.4.4 Convergence results

Strongly convex functions. By Equation (24), when $f_{t,i}(\omega)$ are strongly convex functions, using Lemma A.1, and define $q_t = (1 - \frac{\mu\eta}{2})^{1-t}$, we have

$$f(\omega_F) - f(\omega^*) \leq \mathcal{O} \left(\mu \|\omega_0 - \omega^*\|^2 \exp(-\frac{\mu\eta T}{2}) \right) + \frac{1}{\sum_{t=1}^T q_t} q_t (c_1 \eta + c_2 \eta^2 + \varphi_t).$$

By Lemma A.6, we have

$$\begin{aligned} \frac{1}{\sum_{t=1}^T q_t} \sum_{t=1}^T q_t (c_R + c_{p_G}) &= \frac{1}{\sum_{t=1}^T q_t} \sum_{t=1}^T q_t \left(G^2 + D^2 \left(\frac{D^2+(t-1)R^2}{tD^2+(t-1)R^2} \right) \right) \\ &= \frac{1}{\sum_{t=1}^T q_t} \sum_{t=1}^T q_t \left(G^2 + D^2 \left(\frac{R^2}{R^2+D^2} + \frac{D^4}{(R^2+D^2)^2} \frac{1}{t - \frac{R^2}{R^2+D^2}} \right) \right) \\ &= \mathcal{O} \left(G^2 + D^2 \left(\frac{R^2}{R^2+D^2} + \frac{D^4}{(R^2+D^2)^2} \frac{\ln T}{T} \right) \right). \end{aligned}$$

For φ_t , by Lemma B.4, we have

$$\varphi = \frac{1}{\sum_{t=1}^T q_t} \sum_{t=1}^T q_t \varphi_t \leq \mathcal{O} \left(R \left(\frac{D^2}{D^2+R^2} - \frac{D^4}{(D^2+R^2)^2} \frac{\ln T}{T} \right) \|\omega_0 - \omega^*\| \right).$$

Then define $c_1^o = \frac{1}{\sum_{t=1}^T q_t} \sum_{t=1}^T q_t c_1^t$, $c_2^o = \frac{1}{\sum_{t=1}^T q_t} \sum_{t=1}^T q_t c_2^t$, we have

$$\begin{aligned} f(\omega_F) - f(\omega^*) - \varphi &\leq \mathcal{O} \left(\mu \|\omega_0 - \omega^*\|^2 \exp(-\frac{\mu\eta T}{2}) + c_1^o \eta + c_2^o \eta^2 \right) \\ &= \mathcal{O} \left(\mu \|\omega_0 - \omega^*\|^2 \exp(-\frac{\mu T}{Lc_O}) + \frac{\sigma^2}{\mu NK T} + \frac{c_A}{\mu T} + \frac{c_B}{\mu T^2} + \frac{c_C}{\mu^2 T^2} + \frac{c_D}{\mu^2 T^3} \right), \end{aligned}$$

where $c_O = 1 + A^2 + B^2$, $c_A = G^2 + \frac{D^2 R^2}{R^2+D^2}$, $c_B = \frac{D^6}{(R^2+D^2)^2}$, $c_C = \frac{L\sigma^2}{\eta_g^2 K} + \frac{Lc_A}{\eta_g^2}$, $c_D = \frac{Lc_B}{\eta_g^2}$.

General convex functions. When $f_{t,i}(\omega)$ are general convex functions ($\mu = 0$), directly use Lemma A.2 we get

$$f(\omega_F) - f(\omega^*) - \varphi \leq \mathcal{O} \left(\frac{c_O F}{T} + \sqrt{\frac{\sigma^2 F}{NK T}} + \sqrt{\frac{F c_A}{T}} + \frac{\sqrt{c_B F}}{T} + \sqrt[3]{\frac{c_C F^2}{T^2}} + \frac{\sqrt[3]{c_D F^2}}{T} \right),$$

where $c_O = 1 + A^2 + B^2$, $c_A = G^2 + \frac{D^2 R^2}{R^2+D^2}$, $c_B = \frac{D^6}{(R^2+D^2)^2}$, $c_C = \frac{L\sigma^2}{\eta_g^2 K} + \frac{Lc_A}{\eta_g^2}$, $c_D = \frac{Lc_B}{\eta_g^2}$, and $F = \|\omega_0 - \omega^*\|^2$.

The drift of optimal point. Because of information loss, we can't get the true optimal point when considering previous rounds' information. Instead, the drift can be described as

$$\varphi = c_3^o \|\omega_0 - \omega^*\| = \mathcal{O} \left(R \left(\frac{D^2}{D^2+R^2} - \frac{D^4}{(D^2+R^2)^2} \frac{\ln T}{T} \right) \|\omega_0 - \omega^*\| \right).$$

Convergence of FedAvg. Notice that FedAvg is a special case of CFL by setting $p_{t,i} = 1$ on round t . Having this, we derive the one round convergence of FedAvg under our formulation as

$$f(\boldsymbol{\omega}_t) - f(\boldsymbol{\omega}^*) \leq \frac{1}{\eta}(1 - \frac{\mu\eta}{2})\mathbb{E}\|\boldsymbol{\omega}_t - \boldsymbol{\omega}^*\|^2 - \frac{1}{\eta}\mathbb{E}\|\boldsymbol{\omega}_{t+1} - \boldsymbol{\omega}^*\|^2 + c_1\eta + c_2\eta^2, \quad (24)$$

where $c_1 = 2(G^2 + D^2) + \frac{\sigma^2}{NK}$, $c_2 = \frac{L(G^2+D^2)}{3\eta_g^2} + \frac{L\sigma^2}{6\eta_g^2K}$. Then using Lemma A.1, we get the convergence rate when $f_{t,i}(\boldsymbol{\omega})$ are μ strongly convex

$$f(\boldsymbol{\omega}_t) - f(\boldsymbol{\omega}^*) \leq \mathcal{O}\left(\mu\|\boldsymbol{\omega}_0 - \boldsymbol{\omega}^*\|^2 \exp(\frac{\mu T}{Lc_O}) + \frac{\hat{c}_A}{\mu T} + \frac{\hat{c}_C}{\mu^2 T^2}\right),$$

where $c_O = 1 + A^2 + B^2$, $c_A = G^2 + D^2$, $c_C = \frac{L\sigma^2}{\eta_g^2 K} + \frac{Lc_A}{\eta_g^2}$. Besides, when $f_{t,i}(\boldsymbol{\omega})$ are general convex, we have

$$f(\boldsymbol{\omega}_F) - f(\boldsymbol{\omega}^*) \leq \mathcal{O}\left(\frac{c_O F}{T} + \sqrt{\frac{\sigma^2 F}{NK T}} + \sqrt{\frac{F c_A}{T}} + \sqrt[3]{\frac{c_C F^2}{T^2}}\right),$$

where $c_O = 1 + A^2 + B^2$, $c_A = G^2 + D^2$, $c_C = \frac{L\sigma^2}{\eta_g^2 K} + \frac{Lc_A}{\eta_g^2}$, and $F = \|\boldsymbol{\omega}_0 - \boldsymbol{\omega}^*\|^2$.

B.5 Proof of Convergence Rate for Non-convex Setting

In this section, we present the convergence results for the CFL and FedAvg algorithms under Assumptions 1–4 when the local objective functions $f_{t,i}(\boldsymbol{\omega})$ are not convex. Firstly, based on the definition of an L-smooth function, we have that

$$\mathbb{E}[f(\boldsymbol{\omega}_{t+1})] \leq \mathbb{E}[f(\boldsymbol{\omega}_t)] + \underbrace{\mathbb{E}[\langle \nabla f(\boldsymbol{\omega}_t), \Delta \boldsymbol{\omega}_t \rangle]}_{A_1} + \frac{L}{2} \underbrace{\mathbb{E}[\|\Delta \boldsymbol{\omega}_t\|^2]}_{A_2}. \quad (25)$$

For A_1 part of Inequality (25), we have

$$\begin{aligned} & \mathbb{E}[\langle \nabla f(\boldsymbol{\omega}_t), \Delta \boldsymbol{\omega}_t \rangle] \\ &= \frac{-\eta}{NK} \sum_{i=1}^N \sum_{k=1}^K \mathbb{E}[\langle \nabla f(\boldsymbol{\omega}_t), \nabla \bar{f}_{t,i}(\boldsymbol{\omega}_{t,i,k}) \rangle], \\ &= \frac{-\eta}{NK} \sum_{i=1}^N \sum_{k=1}^K \mathbb{E}\left[\langle \nabla f(\boldsymbol{\omega}_t), \sum_{\tau=1}^t p_{\tau,i} \nabla f_{\tau,i}(\boldsymbol{\omega}_{t,i,k}) - \sum_{\tau=1}^{t-1} p_{\tau,i} \Delta_{\tau,i}(\boldsymbol{\omega}_{t,i,k}) \rangle\right], \\ &\leq \frac{-\eta}{NK} \sum_{i=1}^N \sum_{k=1}^K \mathbb{E}\left[\langle \nabla f(\boldsymbol{\omega}_t), \sum_{\tau=1}^t p_{\tau,i} \nabla f_{\tau,i}(\boldsymbol{\omega}_{t,i,k}) \rangle\right] + \frac{\eta}{2N} \sum_{i=1}^N (1 - p_{t,i}) \left(\mathbb{E}[\|\nabla f(\boldsymbol{\omega}_t)\|^2] + R^2\right), \\ &= \frac{\eta}{2NK} \sum_{i=1}^N \sum_{k=1}^K \left(\mathbb{E}\left[\left\|\nabla f(\boldsymbol{\omega}_t) - \sum_{\tau=1}^t p_{\tau,i} \nabla f_{\tau,i}(\boldsymbol{\omega}_{t,i,k})\right\|^2\right] - \mathbb{E}\left[\left\|\sum_{\tau=1}^t p_{\tau,i} \nabla f_{\tau,i}(\boldsymbol{\omega}_{t,i,k})\right\|^2\right]\right), \\ &+ \frac{\eta}{2N} \sum_{i=1}^N (1 - p_{t,i}) \left(\mathbb{E}[\|\nabla f(\boldsymbol{\omega}_t)\|^2] + R^2\right) - \frac{\eta}{2} \mathbb{E}[\|\nabla f(\boldsymbol{\omega}_t)\|^2]. \end{aligned} \quad (26)$$

From Inequality (14), we have

$$\mathbb{E}[\|\Delta \boldsymbol{\omega}_t\|^2] \leq \frac{2\eta^2}{NK} \sum_{i=1}^N \sum_{k=1}^K \left(\mathbb{E}\left[\left\|\sum_{\tau=1}^t p_{\tau,i} \nabla f_{\tau,i}(\boldsymbol{\omega}_{t,i,k})\right\|^2\right] + \mathbb{E}\left[\left\|\sum_{\tau=1}^{t-1} p_{\tau,i} \Delta_{\tau,i}(\boldsymbol{\omega}_{t,i,k})\right\|^2\right]\right) + \frac{\eta^2 \sigma^2}{NK}. \quad (27)$$

Combine Inequalities (26) and (27), we can observe that when $\eta \leq \frac{1}{2L}$, the $\mathbb{E}\left[\left\|\sum_{\tau=1}^t p_{\tau,i} \nabla f_{\tau,i}(\boldsymbol{\omega}_{t,i,k})\right\|^2\right]$ term can be ignored, since the coefficient number will less than 0. This leaves us with the remaining term in A_2 as $\frac{2\eta^2}{N} \sum_{i=1}^N (1 - p_{t,i})^2 R^2 + \frac{\eta^2 \sigma^2}{NK}$. To address the remaining challenge posed by Inequality (26), we consider the quantity

$$\begin{aligned}
& \left\| \nabla f(\boldsymbol{\omega}_t) - \sum_{\tau=1}^t p_{\tau,i} \nabla f_{\tau,i}(\boldsymbol{\omega}_{t,i,k}) \right\|^2 \\
& \mathbb{E} \left[\left\| \nabla f(\boldsymbol{\omega}_t) - \sum_{\tau=1}^t p_{\tau,i} \nabla f_{\tau,i}(\boldsymbol{\omega}_{t,i,k}) \right\|^2 \right] \\
& = \mathbb{E} \left[\left\| \nabla f(\boldsymbol{\omega}_t) - \nabla f(\boldsymbol{\omega}_{t,i,k}) + \nabla f(\boldsymbol{\omega}_{t,i,k}) - \sum_{\tau=1}^t p_{\tau,i} \nabla f_{\tau,i}(\boldsymbol{\omega}_{t,i,k}) \right\|^2 \right], \\
& \leq 2\mathbb{E} \left[\left\| \nabla f(\boldsymbol{\omega}_t) - \nabla f(\boldsymbol{\omega}_{t,i,k}) \right\|^2 \right] + 2\mathbb{E} \left[\left\| \nabla f(\boldsymbol{\omega}_{t,i,k}) - \sum_{\tau=1}^t p_{\tau,i} \nabla f_{\tau,i}(\boldsymbol{\omega}_{t,i,k}) \right\|^2 \right], \\
& \leq 2L^2 \mathbb{E} \left[\left\| \boldsymbol{\omega}_t - \boldsymbol{\omega}_{t,i,k} \right\|^2 \right] + \left(B^2 + A^2 \sum_{\tau=1}^t p_{\tau,i}^2 \right) \mathbb{E} \left[\left\| \nabla f(\boldsymbol{\omega}_{t,i,k}) \right\|^2 \right] + \left(G^2 + D^2 \sum_{\tau=1}^t p_{\tau,i}^2 \right), \\
& \leq 2L^2 \mathbb{E} \left[\left\| \boldsymbol{\omega}_t - \boldsymbol{\omega}_{t,i,k} \right\|^2 \right] + 2L^2 \left(B^2 + A^2 \sum_{\tau=1}^t p_{\tau,i}^2 \right) \mathbb{E} \left[\left\| \boldsymbol{\omega}_{t,i,k} - \boldsymbol{\omega}_t \right\|^2 \right] \\
& + 2 \left(B^2 + A^2 \sum_{\tau=1}^t p_{\tau,i}^2 \right) \mathbb{E} \left[\left\| \nabla f(\boldsymbol{\omega}_t) \right\|^2 \right] + \left(G^2 + D^2 \sum_{\tau=1}^t p_{\tau,i}^2 \right). \tag{28}
\end{aligned}$$

Combine Inequalities (26) and (28), we have

$$\begin{aligned}
& \mathbb{E} [\langle \nabla f(\boldsymbol{\omega}_t), \Delta \boldsymbol{\omega}_t \rangle] \\
& \leq \frac{\eta L^2}{NK} \sum_{i=1}^N \sum_{k=1}^K c_{p_B,i} \mathbb{E} \left[\left\| \boldsymbol{\omega}_{t,i,k} - \boldsymbol{\omega}_t \right\|^2 \right] + \eta (c_{p_B} - 1 - \frac{\sum_{i=1}^N p_{t,i}}{2N}) \mathbb{E} \left[\left\| \nabla f(\boldsymbol{\omega}_t) \right\|^2 \right] \\
& + \frac{\eta}{2} \left(c_{p_G} + \frac{1}{N} \sum_{i=1}^N (1 - p_{t,i}) R^2 \right). \tag{29}
\end{aligned}$$

Combine Inequalities (25) and (29), we have

$$\begin{aligned}
\mathbb{E} [f(\boldsymbol{\omega}_{t+1})] & \leq \mathbb{E} [f(\boldsymbol{\omega}_t)] + \frac{\eta L^2}{NK} \sum_{i=1}^N \sum_{k=1}^K c_{p_B,i} \mathbb{E} \left[\left\| \boldsymbol{\omega}_{t,i,k} - \boldsymbol{\omega}_t \right\|^2 \right] \\
& + \eta (c_{p_B} - 1 - \frac{\sum_{i=1}^N p_{t,i}}{2N}) \mathbb{E} \left[\left\| \nabla f(\boldsymbol{\omega}_t) \right\|^2 \right] + \frac{\eta}{2} \left(c_{p_G} + \frac{1}{N} \sum_{i=1}^N (1 - p_{t,i}) R^2 \right) \\
& + \frac{L\eta^2}{N} \sum_{i=1}^N (1 - p_{t,i})^2 R^2 + \frac{L\eta^2 \sigma^2}{2NK}.
\end{aligned}$$

By Inequalities (17) and (18), we have

$$\begin{aligned}
& \mathbb{E} \left\| \boldsymbol{\omega}_{t,i,k} - \boldsymbol{\omega}_t \right\|^2 \\
& \leq 4k^2 \eta_i^2 L^2 c_{p_B,i} \mathbb{E} \left\| \boldsymbol{\omega}_{t,i,k-1} - \boldsymbol{\omega}_t \right\|^2 + 4k^2 \eta_i^2 c_{p_B,i} (\mathbb{E} \left[\left\| \nabla f(\boldsymbol{\omega}_t) \right\|^2 \right]) + 2k^2 \eta_i^2 c_{p_G,i} \\
& + 2k^2 \eta_i^2 (\sum_{\tau=1}^{t-1} p_{\tau,i})^2 R^2 + k\eta_i^2 \sigma^2. \tag{30}
\end{aligned}$$

By iteratively applying Inequality (30), we obtain

$$\begin{aligned}
& \mathbb{E} \left\| \boldsymbol{\omega}_{t,i,k} - \boldsymbol{\omega}_t \right\|^2 \\
& \leq \sum_{r=0}^{k-1} \left(4k^2 \eta_i^2 c_{p_B,i} (\mathbb{E} \left[\left\| \nabla f(\boldsymbol{\omega}_t) \right\|^2 \right]) + 2k^2 \eta_i^2 c_{p_G,i} + 2k^2 \eta_i^2 (\sum_{\tau=1}^{t-1} p_{\tau,i})^2 R^2 + k\eta_i^2 \sigma^2 \right) (4k^2 \eta_i^2 L^2 c_{p_B,i})^r, \\
& \leq \frac{(4k^2 \eta_i^2 c_{p_B,i} (\mathbb{E} \left[\left\| \nabla f(\boldsymbol{\omega}_t) \right\|^2 \right]) + 2k^2 \eta_i^2 c_{p_G,i} + 2k^2 \eta_i^2 (\sum_{\tau=1}^{t-1} p_{\tau,i})^2 R^2 + k\eta_i^2 \sigma^2)}{1 - 4k^2 \eta_i^2 L^2 c_{p_B,i}}.
\end{aligned}$$

Let $8K^2 \eta_i^2 c_{p_B,i} \leq 1$, we have

$$\begin{aligned}
& \frac{1}{NK} \sum_{i=1}^N \sum_{k=1}^K c_{p_B,i} \mathbb{E} \left\| \boldsymbol{\omega}_{t,i,k-1} - \boldsymbol{\omega}_t \right\|^2 \\
& \leq \frac{1}{N} \sum_{i=1}^N c_{p_B,i} \frac{(4K^2 \eta_i^2 c_{p_B,i} (\mathbb{E} \left[\left\| \nabla f(\boldsymbol{\omega}_t) \right\|^2 \right]) + 2K^2 \eta_i^2 c_{p_G,i} + 2K^2 \eta_i^2 (\sum_{\tau=1}^{t-1} p_{\tau,i})^2 R^2 + K\eta_i^2 \sigma^2)}{1 - 4K^2 \eta_i^2 L^2 c_{p_B,i}}, \\
& \leq \frac{1}{N} \sum_{i=1}^N c_{p_B,i} \mathbb{E} \left[\left\| \nabla f(\boldsymbol{\omega}_t) \right\|^2 \right] + \frac{1}{2} c_{p_G,i} + \frac{1}{2} (\sum_{\tau=1}^{t-1} p_{\tau,i})^2 R^2 + \frac{\sigma^2}{4K}, \\
& = c_{p_B} \mathbb{E} \left[\left\| \nabla f(\boldsymbol{\omega}_t) \right\|^2 \right] + \frac{1}{2} c_{p_G} + \frac{1}{2N} \sum_{i=1}^N (\sum_{\tau=1}^{t-1} p_{\tau,i})^2 R^2 + \frac{\sigma^2}{4K}. \tag{31}
\end{aligned}$$

Then combine Inequalities (25), (27), (29), and (31), we have

$$\begin{aligned}
\mathbb{E} [f(\boldsymbol{\omega}_{t+1})] & \leq \mathbb{E} [f(\boldsymbol{\omega}_t)] + \eta \left((L^2 + 1) c_{p_B} - 1 - \frac{\sum_{i=1}^N p_{t,i}}{2N} \right) \mathbb{E} \left[\left\| \nabla f(\boldsymbol{\omega}_t) \right\|^2 \right] \\
& + \frac{\eta}{2} \left(c_{p_G} + \frac{1}{N} \sum_{i=1}^N (1 - p_{t,i}) R^2 \right) + \frac{L\eta^2}{N} \sum_{i=1}^N (1 - p_{t,i})^2 R^2 + \frac{L\eta^2 \sigma^2}{2NK} \\
& + \eta L^2 \left(\frac{1}{2} c_{p_G} + \frac{1}{2N} \sum_{i=1}^N (\sum_{\tau=1}^{t-1} p_{\tau,i})^2 R^2 + \frac{\sigma^2}{4K} \right). \tag{32}
\end{aligned}$$

Then we must to choose the value of $p_{t,i}$ for better convergence. Follow the idea that we want to train a better model when convergent, we choose $p_{t,i}$ that can minimize the constant term, which is by solving

$$\min_p G^2 + D^2 \sum_{\tau=1}^t p_{\tau,i}^2 + (\sum_{\tau=1}^{t-1} p_{\tau,1})^2 R^2, s.t. \sum_{\tau=1}^t p_{\tau,1} = 1.$$

We get same results as when the objective function is convex, that is, $p_{\tau,i} = \frac{D^2}{tD^2+(t-1)R^2}$ for any $\tau < t$, and $p_{t,i} = \frac{(t-1)R^2+D^2}{tD^2+(t-1)R^2}$, and $\min\{G^2 + D^2 \sum_{\tau=1}^t p_{\tau,i}^2 + (\sum_{\tau=1}^{t-1} p_{\tau,1})^2 R^2\} = G^2 + D^2 \left(\frac{D^2+(t-1)R^2}{tD^2+(t-1)R^2} \right)$. Then we simplify the equation by using $c_0(t)$, $c_1(t)$, and $c_2(t)$ to denote the constant terms, we have

$$\mathbb{E}[f(\omega_{t+1})] \leq \mathbb{E}[f(\omega_t)] - \eta c_0(t) \mathbb{E}[\|\nabla f(\omega_t)\|^2] + \eta c_1(t) + \eta^2 c_2(t)$$

Moving $\mathbb{E}[\|\nabla f(\omega_t)\|^2]$ term to the left, we have

$$\frac{1}{T} \sum_{t=1}^T c_0(t) \mathbb{E}[\|\nabla f(\omega_t)\|^2] \leq \frac{\mathbb{E}[f(\omega_0)] - \mathbb{E}[f(\omega^*)]}{\eta} + \eta \frac{1}{T} \sum_{t=1}^T c_2(t) + \varphi$$

Consider c_0 , because the value of B^2 and A can't be constrained, the algorithm can't converge for very large A and B . Here we first consider when $c_0 < 0$, and use c_m to denote the min c_0 . Then let $\eta = \frac{\sqrt{KN}}{\sqrt{TL}}$, we derive the convergence rate as

$$\begin{aligned} \frac{1}{T} \sum_{t=1}^T \mathbb{E}[\|\nabla f(\omega_t)\|^2] &= O\left(\frac{L(f_0-f_*)}{\sqrt{TNK}c_m} + \frac{1}{\sqrt{T}} \left(\frac{\sqrt{KN}}{L} \left(\frac{R^2}{R^2+D^2} \right)^2 + \frac{\sigma^2}{\sqrt{NK}} \right) \right) \\ &\quad + \frac{\sqrt{KN}}{TL} \frac{D^4}{c_m(R^2+D^2)^2} + \frac{\sqrt{KN}}{T\sqrt{TL}} \left(\frac{D^4}{(R^2+D^2)^2} \right)^2 \end{aligned}$$

Then we want to analyse when the algorithm won't converge. When the algorithm won't converge, that means $c_0 \geq 0$. Because $c_0 = (L^2 + 1)c_{p_B} - 1 - \frac{\sum_{i=1}^N p_{t,i}}{2N} = \frac{1}{N} \sum_{i=1}^N (L^2 + 1)(1 + A^2 + B^2 \sum_{\tau=1}^t p_{\tau,i}^2) - 1 - \frac{p_{t,i}}{2}$. Then the value of A^2, B^2, L, p decide if $c_0 \geq 0$.

Notice that in FedAvg, $p_{t,i} = 1$, and $c_{0,avg} = (L^2 + 1)(1 + A^2 + B^2) - \frac{3}{2}$, and in CFL, we can setting different p to get better convergence. For example, when B is large, setting $p_{\tau,i} = \frac{1}{t}$, we have $c_0 = (L^2 + 1)(1 + A^2 + \frac{B^2}{t}) - 1 - \frac{1}{2t}$. Thus, we draw the conclusion as

Then we have following observations:

- *CFL converge faster than FedAvg by reducing the variance terms.* For $c_0 = \frac{1}{N} \sum_{i=1}^N (L^2 + 1)(1 + A^2 + B^2 \sum_{\tau=1}^t p_{\tau,i}^2) - 1 - \frac{p_{t,i}}{2}$, in FedAvg, we have $p_{t,i} = 1$, then $c_{0,avg} = (L^2 + 1)(1 + A^2 + B^2) - \frac{3}{2}$. However, in CFL, we can adjust p , such as when setting $p_{\tau,i} = \frac{1}{t}$, we have $c_0 = (L^2 + 1)(1 + A^2 + \frac{B^2}{t}) - 1 - \frac{1}{2t}$, then the variance term reduce from B^2 to $\frac{B^2}{t}$.
- *The convergence rate of CFL become better for larger t , since c_{p_B} in c_0 become smaller for larger t .*
- *Improve N, K will speed up the convergence by reducing the terms about $f_0 - f_*$ and σ^2 . However, larger N and K will cause larger information loss and round drift (terms with R and D), thus, it should be a trade off in practice.*

B.6 Theoretical Results

We give the full version of Convergence results as follows.

Theorem B.5 (Convergence rate of CFL methods). *Assume $\{f_{t,i}(\omega)\}$ satisfy Assumption 1–4, the output of Algorithm 1 has expected error smaller than $\epsilon + \varphi$, for $\eta_g = 1, \eta_l \leq \frac{\sqrt{3+4(1+B^2+A^2)} - \sqrt{4(1+B^2+A^2)}}{6KL\sqrt{1+B^2+A^2}}$, $p_{\tau,i} = \frac{D^2}{tD^2+(t-1)R^2}$ ($\tau < t$), and $p_{t,i} = \frac{(t-1)R^2+D^2}{tD^2+(t-1)R^2}$ on round t .*

When $\{f_{t,i}(\omega)\}$ are μ -strongly convex functions, we have

$$T = O\left(\frac{Lc_0}{\mu} + \frac{\sigma^2}{\mu NK\epsilon} + \frac{c_A}{\mu\epsilon} + \sqrt{\frac{c_B}{\mu\epsilon}} + \sqrt{\frac{c_C}{\mu^2\epsilon}} + \sqrt[3]{\frac{c_D}{\mu^2\epsilon}}\right),$$

and when $\{f_{t,i}(\omega)\}$ are general convex functions ($\mu = 0$), we have

$$T = \mathcal{O} \left(\frac{c_O \mathcal{H} + \sqrt{c_B \mathcal{H}} + \sqrt[3]{c_D \mathcal{H}^2}}{\epsilon} + \frac{\sigma^2 \mathcal{H}}{NK \epsilon^2} + \frac{c_A \mathcal{H}}{\epsilon^2} + \sqrt{\frac{c_C \mathcal{H}^2}{\epsilon^3}} \right),$$

and when $\{f_{t,i}(\omega)\}$ are non-convex, setting $\eta = K \eta_g \eta_l = \frac{\sqrt{KN}}{\sqrt{TL}}$, when $\frac{1}{T} \sum_{t=1}^T \mathbb{E} \left[\|\nabla f(\omega_t)\|^2 \right]$ reach ϵ we have

$$T = \mathcal{O} \left(\frac{L^2(f_0 - f_*)^2}{NK c_m^2 \epsilon^2} + \frac{1}{\epsilon^2} \left(\frac{\sqrt{KN} c_{R1}}{L} + \frac{\sigma^2}{\sqrt{NK}} \right)^2 + \frac{\sqrt{KN} c_{R2}}{c_m \epsilon L} \right),$$

where $c_O = 1 + A^2 + B^2$, $c_A = G^2 + \frac{D^2 R^2}{R^2 + D^2}$, $c_B = \frac{D^6}{(R^2 + D^2)^2}$, $c_C = \frac{L \sigma^2}{\eta_g^2 K} + \frac{L c_A}{\eta_g^2}$, $c_D = \frac{L c_B}{\eta_g^2}$, $c_{R1} = \frac{R^2}{R^2 + D^2}$, $c_{R2} = \frac{D^4}{(R^2 + D^2)^2}$, c_m is a constant related to A, B and R , and $\mathcal{H} = \|\omega_0 - \omega^*\|^2$. N is the number of chosen clients in each round, and K is the number of local iterations.

Theorem B.6 (Convergence rate of FedAvg under time-varying scenarios). Assume $\{f_{t,i}(\omega)\}$ satisfy Assumption 1–4, the output of FedAvg has expected error smaller than ϵ , for $\eta_g = 1$ and $\eta_l \leq \frac{\sqrt{3+4(1+B^2+A^2)} - \sqrt{4(1+B^2+A^2)}}{6KL\sqrt{1+B^2+A^2}}$. When $\{f_{t,i}(\omega)\}$ are μ -strongly convex functions, we have

$$T = \mathcal{O} \left(\frac{L c_O}{\mu} + \frac{\sigma^2}{\mu NK \epsilon} + \frac{c_A}{\mu \epsilon} + \sqrt{\frac{c_C}{\mu^2 \epsilon}} \right),$$

and when $\{f_{t,i}(\omega)\}$ are general convex functions ($\mu = 0$), we have

$$T = \mathcal{O} \left(\frac{c_O \mathcal{H}}{\epsilon} + \frac{\sigma^2 \mathcal{H}}{NK \epsilon^2} + \frac{c_A \mathcal{H}}{\epsilon^2} + \sqrt{\frac{c_C \mathcal{H}^2}{\epsilon^3}} \right),$$

and when $\{f_{t,i}(\omega)\}$ are non-convex, setting $\eta = K \eta_g \eta_l = \frac{\sqrt{KN}}{\sqrt{TL}}$, when $\frac{1}{T} \sum_{t=1}^T \mathbb{E} \left[\|\nabla f(\omega_t)\|^2 \right]$ reach ϵ we have

$$T = \mathcal{O} \left(\frac{L^2(f_0 - f_*)^2}{NK c_m^2 \epsilon^2} + \frac{1}{\epsilon^2} \left(\frac{\sqrt{KN}}{L} + \frac{\sigma^2}{\sqrt{NK}} \right)^2 \right),$$

where $c_O = 1 + A^2 + B^2$, $c_A = G^2 + D^2$, $c_C = \frac{L \sigma^2}{\eta_g^2 K} + \frac{L c_A}{\eta_g^2}$, and $\mathcal{H} = \|\omega_0 - \omega^*\|^2$. N is the number of chosen clients in each round, and K is the number of local iterations.

B.7 Convergence Rate of CFL under Correlated Time Drifts

In this section, we study the scenario where the time drifts $\xi_{t_1,i}$ and $\xi_{t_2,i}$ are correlated. We first provide some useful lemmas.

Lemma B.7 (Bounded Gradient Noise of CFL under correlated time drifts). For Formulation (2), consider CFL and FedAvg, when time drift $\xi_{t,i}$ satisfy Assumption 6, we can bound the gradient drift as

$$\begin{aligned} \mathbb{E} \left\| \sum_{\tau=1}^t p_{\tau,i} \nabla f_{\tau,i}(\omega) \right\|^2 &\leq \left(1 + B^2 + A^2 \sum_{\tau=1}^t p_{\tau,i}^2 + C^2 \sum_{\tau_1 \neq \tau_2}^t p_{\tau_1,i} p_{\tau_2,i} \right) \mathbb{E} \|\nabla f(\omega)\|^2 \\ &\quad + G^2 + D^2 \sum_{\tau=1}^t p_{\tau,i}^2 + \min(F^2, D^2) \sum_{\tau_1 \neq \tau_2}^t p_{\tau_1,i} p_{\tau_2,i}. \end{aligned}$$

Proof. Using Assumption 3, together with the fact that $\nabla f_{t,i}(\omega) = \nabla f(\omega) + \delta_{t,i} + \xi_{t,i}$ (Here to simplify the notation, we use $\{t, i\}$ pair to denote the client participate in training on round t and number i), we have

$$\begin{aligned} \mathbb{E} \left\| \sum_{\tau=1}^t p_{\tau,i} \nabla f_{\tau,i}(\omega) \right\|^2 &= \mathbb{E} \left\| \sum_{\tau=1}^t p_{\tau,i} (\nabla f_{\tau,i}(\omega) + \delta_i + \xi_{\tau,i}) \right\|^2, \\ &= \mathbb{E} \|\nabla f(\omega)\|^2 + \mathbb{E} \|\delta_i\|^2 + \mathbb{E} \left\| \sum_{\tau=1}^t p_{\tau,i} \xi_{\tau,i} \right\|^2, \\ &\leq \left(1 + B^2 + A^2 \sum_{\tau=1}^t p_{\tau,i}^2 + C^2 \sum_{\tau_1 \neq \tau_2}^t p_{\tau_1,i} p_{\tau_2,i} \right) \mathbb{E} \|\nabla f(\omega)\|^2 \\ &\quad + G^2 + D^2 \sum_{\tau=1}^t p_{\tau,i}^2 + \min(F^2, D^2) \sum_{\tau_1 \neq \tau_2}^t p_{\tau_1,i} p_{\tau_2,i}. \end{aligned}$$

□

Based on the results of Inequalities (15) and (20), we define $c_{pB,i} = 1 + B^2 + A^2 \sum_{\tau=1}^t p_{\tau,i}^2 + C^2 \sum_{\tau_1 \neq \tau_2}^t p_{\tau_1,i} p_{\tau_2,i}$, and $c_{pG,i} = G^2 + D^2 \sum_{\tau=1}^t p_{\tau,i}^2 + F^2 \sum_{\tau_1 \neq \tau_2}^t p_{\tau_1,i} p_{\tau_2,i}$. This leads to the same results as Inequality (24). The difference between using Lemma 3 and Lemma B.7 is only in the definitions of $c_{pB,i}$ and $c_{pG,i}$. As in Section B.4.3, the optimal weights can be found by solving the following optimization problem

$$\begin{aligned} \min_p \frac{1}{N} \sum_{i=1}^N (1 - p_{t,i})^2 R^2 + G^2 + D^2 \left(\sum_{\tau=1}^t p_{\tau,i}^2 \right) + \min(F^2, D^2) \sum_{\tau_1 \neq \tau_2}^t p_{\tau_1} p_{\tau_2}, \\ \text{s.t. } \sum_{\tau=1}^t p_{\tau,i} = 1, \forall i = 1, \dots, N. \end{aligned} \tag{33}$$

Then we can get,

$$p_{\tau,i} = \frac{\max(D^2 - F^2, 0)}{t \max(D^2 - F^2, 0) + (t-1)R^2}, \forall \tau < t, p_{t,i} = \frac{(t-1)R^2 + \max(D^2 - F^2, 0)}{t \max(D^2 - F^2, 0) + (t-1)R^2}.$$

Compare with the results in Section B.4.3, we can found that the weights when using Lemma B.7 is the same as the weights of using Lemma 3, and set D^2 to $\max(D^2 - F^2, 0)$. Then substitute the $p_{\tau,i}$ and $p_{t,i}$ in Section B.4.4 and Section B.5, we derive the convergence rate under Assumption 6.

Theorem B.8 (Convergence rate of CFL methods under correlated time drifts). *Assume $\{f_{t,i}(\omega)\}$ satisfy Assumption 1–6, the output of Algorithm 1 has expected error smaller than $\epsilon + \varphi$, for $\eta_g = 1$, $\eta_l \leq \frac{\sqrt{3+4c_O} - \sqrt{4c_O}}{6KL\sqrt{c_O}}$, $p_{\tau,i} = \frac{M^2}{t(M^2) + (t-1)R^2}$ (for $\tau < t$), and $p_{t,i} = \frac{(t-1)R^2 + M^2}{t(M^2) + (t-1)R^2}$ on round t .*

When $\{f_{t,i}(\omega)\}$ are μ -strongly convex functions, we have,

$$T = \mathcal{O} \left(\frac{Lc_O}{\mu} + \frac{\sigma^2}{\mu NK\epsilon} + \frac{1}{\mu\epsilon} \left(G^2 + \frac{M^2 R^2}{R^2 + M^2} \right) \right),$$

and when $\{f_{t,i}(\omega)\}$ are general convex functions ($\mu = 0$), we have

$$T = \mathcal{O} \left(\frac{c_O \mathcal{H}}{\epsilon} + \frac{\sigma^2 \mathcal{H}}{NK\epsilon^2} + \frac{\mathcal{H}}{\epsilon^2} \left(G^2 + \frac{M^2 R^2}{R^2 + M^2} \right) \right),$$

and when $\{f_{t,i}(\omega)\}$ are non-convex, by setting $\eta = K\eta_g\eta_l = \frac{\sqrt{KN}}{\sqrt{TL}}$, $\frac{1}{T} \sum_{t=1}^T \mathbb{E} \left[\|\nabla f(\omega_t)\|^2 \right]$ needs to take the following steps to reach ϵ

$$T = \mathcal{O} \left(\frac{L^2(f_0 - f_*)^2}{NKc_m^2\epsilon^2} + \frac{1}{\epsilon^2} \left(\frac{\sqrt{KN}c_{R1}^2}{L} + \frac{\sigma^2}{\sqrt{NK}} \right)^2 \right),$$

where $M^2 = \max(0, D^2 - F^2)$, $c_O = 1 + A^2 + \max(B^2, C^2)$, $c_{R1} = \frac{R^2}{R^2 + M^2}$, c_m is a constant related to A , B , C and R , and $\mathcal{H} = \|\omega_0 - \omega^*\|^2$. N is the number of chosen clients in each round, and K is the number of local iterations.

B.8 Proof of Theorem 7

Lemma B.9. *Given*

$$Q = \begin{bmatrix} D^2 + R^2 & \alpha D^2 + R^2 & \dots & \alpha^{t-2} D^2 + R^2 & \alpha^{t-1} D^2 \\ \alpha D^2 + R^2 & D^2 + R^2 & \dots & \alpha^{t-3} D^2 + R^2 & \alpha^{t-2} D^2 \\ \vdots & \vdots & & \vdots & \vdots \\ \alpha^{t-2} D^2 + R^2 & \alpha^{t-3} D^2 + R^2 & \dots & \alpha^2 D^2 + R^2 & \alpha D^2 \\ \alpha^{t-1} D^2 & \alpha^{t-2} D^2 & \dots & \alpha D^2 & D^2 \end{bmatrix}, \quad (34)$$

we have Q is positive definite.

Proof. We can decompose Q into two matrix, M_R and M_F , and $Q = M_R + M_F$. Firstly, we would like to show that M_R is positive and semi-definite, and M_R is defined by,

$$M_R = \begin{bmatrix} R^2 & R^2 & \dots & R^2 & 0 \\ R^2 & R^2 & \dots & R^2 & 0 \\ \vdots & \vdots & & \vdots & \vdots \\ R^2 & R^2 & \dots & R^2 & 0 \\ 0 & 0 & \dots & 0 & 0 \end{bmatrix}.$$

First, let us consider the matrix M_R . It has a rank of 1 and $t - 1$ zero eigenvalues, with a single non-zero eigenvalue of $(t - 1)R^2$. This means that M_R is positive and semi-definite. Next, we will prove that M_F is positive definite. This matrix is defined as follows

$$M_F = \begin{bmatrix} D^2 & \alpha D^2 & \dots & \alpha^{t-2} D^2 & \alpha^{t-1} D^2 \\ \alpha D^2 & D^2 & \dots & \alpha^{t-3} D^2 & \alpha^{t-2} D^2 \\ \vdots & \vdots & & \vdots & \vdots \\ \alpha^{t-2} D^2 & \alpha^{t-3} D^2 & \dots & \alpha^2 D^2 & \alpha D^2 \\ \alpha^{t-1} D^2 & \alpha^{t-2} D^2 & \dots & \alpha D^2 & D^2 \end{bmatrix}.$$

By row operations, we can transform M_F into

$$\begin{bmatrix} D^2 & \alpha D^2 & \cdots & \alpha^{t-2} D^2 & \alpha^{t-1} D^2 \\ 0 & D^2(1-\alpha^2) & \cdots & D^2(\alpha^{t-3}-\alpha^{t-1}) & D^2(\alpha^{t-2}-\alpha^t) \\ \vdots & \vdots & & \vdots & \vdots \\ 0 & 0 & \cdots & D^2(1-\alpha^2) & D^2(\alpha-\alpha^3) \\ 0 & 0 & \cdots & 0 & D^2(1-\alpha^2) \end{bmatrix}.$$

Because $0 \leq \alpha < 1$, we have M_F is positive definite. Then $Q = M_R + M_F$ is also positive definite. \square

Lemma B.10 (Bounded Gradient Noise of CFL under correlated time drifts). *For Formulation (2), consider CFL and FedAvg, when time drift $\xi_{t,i}$ satisfy Assumption 5, we can bound the gradient drift as*

$$\begin{aligned} \mathbb{E} \left\| \sum_{\tau=1}^t p_{\tau,i} \nabla f_{\tau,i}(\boldsymbol{\omega}) \right\|^2 &\leq \left(1 + B^2 + A^2 \sum_{\tau=1}^t p_{\tau,i}^2 + \sum_{\tau_1 \neq \tau_2}^t C_{\tau_1, \tau_2}^2 p_{\tau_1, i} p_{\tau_2, i} \right) \mathbb{E} \|\nabla f(\boldsymbol{\omega})\|^2 \\ &\quad + G^2 + D^2 \sum_{\tau=1}^t p_{\tau,i}^2 + \sum_{\tau_1 \neq \tau_2}^t \min(F_{\tau_1, \tau_2}^2, D^2) p_{\tau_1, i} p_{\tau_2, i}. \end{aligned}$$

Proof. Using Assumption 5, together with the fact that $\nabla f_{t,i}(\boldsymbol{\omega}) = \nabla f(\boldsymbol{\omega}) + \boldsymbol{\delta}_{t,i} + \boldsymbol{\xi}_{t,i}$ (Here to simplify the notation, we use $\{t, i\}$ pair to denote the client participate in training on round t and number i), we have

$$\begin{aligned} \mathbb{E} \left\| \sum_{\tau=1}^t p_{\tau,i} \nabla f_{\tau,i}(\boldsymbol{\omega}) \right\|^2 &= \mathbb{E} \left\| \sum_{\tau=1}^t p_{\tau,i} (\nabla f_{\tau,i}(\boldsymbol{\omega}) + \boldsymbol{\delta}_{\tau,i} + \boldsymbol{\xi}_{\tau,i}) \right\|^2, \\ &= \mathbb{E} \|\nabla f(\boldsymbol{\omega})\|^2 + \mathbb{E} \|\boldsymbol{\delta}_i\|^2 + \mathbb{E} \left\| \sum_{\tau=1}^t p_{\tau,i} \boldsymbol{\xi}_{\tau,i} \right\|^2, \\ &\leq \left(1 + B^2 + A^2 \sum_{\tau=1}^t p_{\tau,i}^2 + \sum_{\tau_1 \neq \tau_2}^t C_{\tau_1, \tau_2}^2 p_{\tau_1, i} p_{\tau_2, i} \right) \mathbb{E} \|\nabla f(\boldsymbol{\omega})\|^2 \\ &\quad + G^2 + D^2 \sum_{\tau=1}^t p_{\tau,i}^2 + \sum_{\tau_1 \neq \tau_2}^t \min(F_{\tau_1, \tau_2}^2, D^2) p_{\tau_1, i} p_{\tau_2, i}. \end{aligned}$$

\square

Based on Lemma B.10, using the same process in Section B.7, we can prove that the optimal $p_{\tau,i}$ is given by solving the following optimization problem.

$$\begin{aligned} \min_p \frac{1}{N} \sum_{i=1}^N (1 - p_{t,i})^2 R^2 + G^2 + D^2 (\sum_{\tau=1}^t p_{\tau,i}^2) + \sum_{\tau_1 \neq \tau_2}^t \min(F_{\tau_1, \tau_2}^2, D^2) p_{\tau_1} p_{\tau_2}, \\ \text{s.t. } \sum_{\tau=1}^t p_{\tau,i} = 1, \forall i = 1, \dots, N. \end{aligned}$$

When under Assumption 7, we can change this optimization problem to,

$$\begin{aligned} \min_p \frac{1}{N} \sum_{i=1}^N (1 - p_{t,i})^2 R^2 + G^2 + D^2 \sum_{\tau_1, \tau_2}^t \alpha^{|\tau_1 - \tau_2|} p_{\tau_1} p_{\tau_2}, \\ \text{s.t. } \sum_{\tau=1}^t p_{\tau,i} = 1, \forall i = 1, \dots, N. \end{aligned}$$

This optimization problem can be further transformed to,

$$\begin{aligned} \min_p \frac{1}{N} \sum_{i=1}^N \sum_{\tau_1, \tau_2}^t \alpha^{|\tau_1 - \tau_2|} D^2 p_{\tau_1} p_{\tau_2} + \sum_{\tau_1, \tau_2}^{t-1} R^2 p_{\tau_1} p_{\tau_2}, \\ \text{s.t. } \sum_{\tau=1}^t p_{\tau,i} = 1, \forall i = 1, \dots, N. \end{aligned}$$

Then we can construct a matrix $Q \in \mathbb{R}^{t \times t}$, where $Q_{ij} = \alpha^{|i-j|D^2+R^2}$ for $i, j < t$, and $Q_{ij} = \alpha^{|i-j|D^2}$ for others, then the optimization problem become,

$$\min_{\hat{p}} \hat{p}^T Q \hat{p}, \text{ s.t. } \sum_{\tau=1}^t p_{\tau,i} = 1, \forall i = 1, \dots, N,$$

where $\hat{p} \in \mathbb{R}^t = [p_1, \dots, p_t]^T$. Based on Lemma B.9, we have Q is positive definite, and based on the quadratic programming theory, we can transform the optimization problem to the following linear system,

$$\begin{bmatrix} Q & \mathbf{1} \\ \mathbf{1}^T & 0 \end{bmatrix} \begin{bmatrix} \hat{p} \\ \lambda \end{bmatrix} = \begin{bmatrix} \mathbf{0} \\ 1 \end{bmatrix},$$

where λ is a set of Lagrange multipliers which come out of the solution alongside \hat{p} .

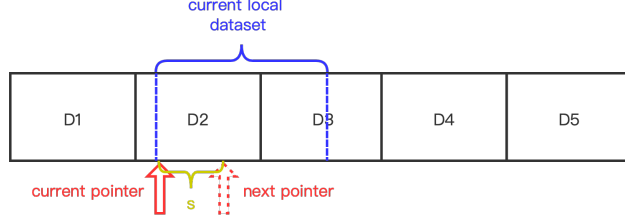


Figure 4: Process of constructing local data sets with overlap. Blue lines bound the current local data sets. Red pointer points to the start of current local data set.

C Experiment details

C.1 Realistic Data Sets

C.1.1 Setup

We consider federated learning an image classifier on split-CIFAR10 and split-CIFAR100 data sets with ResNet18, and split-Fashion-MNIST data set with a two-layer MLP. The “split” follows the idea introduced in previous works (Yurochkin et al., 2019; Hsu et al., 2019; Reddi et al., 2021), where we leverage the Latent Dirichlet Allocation (LDA) to control the distribution drift with parameter α (See Algorithm 6). Larger α denotes smaller drifts here.

In our experiments, unless specifically mentioned otherwise all data sets are partitioned to 210 subsets for 7 different clients: all clients are selected and trained for 500 communication rounds, and each client samples one of the corresponding 30 subsets randomly for the local training. Note that unless mentioned otherwise the training strategy here applies to all FL baselines and CFL methods, and we evaluate the performance of models on global test data sets. We carefully tuned the hyper-parameters in all algorithms, and we report the results under the optimal settings after many trials. For CFL-Regularization, we set the weight of regularization term for $\beta = 1$ on fc layer, and $\beta = 0.1$ for last block (layer). For FedProx, we set the weight of proximal term $\mu = 0.1$, and for MimeLite, we set the global momentum weight for $\gamma = 0.01$. Besides, for all experiments, we set fixed learning rate $lr = 0.01$. We also naively examined warm-up tuning strategies but can not observe significant improvement on final results.

Construct local data sets with overlap. Follow the partition methods of disjoint local data sets; we first split the whole data set to $M \times S$ subsets for S different clients: each client has M disjoint local subsets, and we put these M subsets in sequence. For each client, we use a pointer to point to the start position of the current local data set. Figure 4 show the case when $M = 5$: $D_1 - D_5$ are 5 disjoint local subsets of client i . The pointer point to the start point of a local data set of the current round and the blue lines bound current subsets. At the beginning of training, pointers belong to each client will point to the beginning of the sequence. At the end of each round, the pointer moves s steps, and if it moves to the end of all the sequence, it will come back to the start point.

In practice, the Cifar10 data set is partitioned to 210 subsets for 7 clients, and set the size of local data set $S_l = 285$. Then when we set $s = 285$, the local data sets are disjoint, which means the overlap is 0%. Otherwise, when set $s = 213$, the overlap is 25%, and when set $s = 142$, the overlap is 50%.

C.1.2 Approximation Methods

Regularization Methods. We use Taylor Extension to approximate the objective functions of previous rounds, that is

$$\tilde{f}(\omega) = f(\hat{\omega}) + \nabla f(\hat{\omega})^T(\omega - \hat{\omega}) + \frac{1}{2}(\omega - \hat{\omega})^T \nabla^2 f(\hat{\omega})(\omega - \hat{\omega}),$$

where $\hat{\omega}$ are the parameters of previous rounds. Then the gradient of $\tilde{f}(\omega)$ is

$$\nabla \tilde{f}(\omega) = \nabla f(\hat{\omega}) + \nabla^2 f(\hat{\omega})(\omega - \hat{\omega}).$$

Having this, we can approximate the gradients of objective functions of previous rounds. The problem is how to approximate $\nabla^2 f(\hat{\omega})$. Here we use two kinds of methods to calculate the Hessian matrices. The first is to use the Fisher Information Matrix as introduced in EWC (Kirkpatrick et al., 2017). The Fisher Information Matrix is equal to the diagonal Hessian matrix when using cross entropy loss functions. The Fisher Information Matrix can be calculated by

$$F_{ij} = [\nabla f(\hat{\omega})]_{ij}^2,$$

where F_{ij} are the entries of Fisher Information Matrix. Another method is to calculate the diagonal Hessian matrix. We use the PyHessian package (Yao et al., 2020) in this experiment.

Algorithm 3 iCaRL Construct Core Set

Require: Image set $\mathbf{X} = \{\mathbf{x}_1, \mathbf{x}_2, \mathbf{x}_3, \dots, \mathbf{x}_n\}$ of class y , m : target number of samples, $\phi : \mathcal{X} \rightarrow \mathcal{R}^d$: current feature function

- 1: $\mu \leftarrow \frac{1}{n} \sum_{\mathbf{x} \in \mathbf{X}} \phi(\mathbf{x})$
 - 2: **for** $k = 1, \dots, m$ **do**
 - 3: $p_k \leftarrow \arg \min_{\mathbf{x} \in \mathbf{X}} \left\| \mu - \frac{1}{k} \left(\phi(\mathbf{x}) + \sum_{j=1}^{k-1} \phi(p_j) \right) \right\|$
 - 4: $P \leftarrow (p_1, p_2, \dots, p_m)$
-

| Scenarios | FL baselines | | | | CFL methods | |
|-------------------|--------------|---------|----------|----------|--------------------|--------------|
| | FedAvg | FedProx | SCAFFOLD | MimeLite | CFL-Regularization | CFL-Core-Set |
| Stateful clients | ✓ | ✓ | × | ✓ | ✓ | ✓ |
| Stateless clients | ✓ | ✓ | × | ✓ | ✓ | × |

Table 8: *The applicability of various algorithms under different time-varying scenarios.*

In each round, the server will collect Hessian matrices from clients, and store them in a buffer. Then at the beginning of next round, server combine send latest 40 Hessian matrices, gradients, and parameters, and send them to chosen clients. Each clients use these to calculate regularization terms.

In practice, we only add regularization terms to the top layers (last block and fc layer of ResNet18). This is based on the assumption that top layers contain more personal information while bottom layers contain more general information. We verified that this strategy perform better than adding regularization terms to all layers in experiments.

Generation Methods. We use MCMC to generate samples in each round. In practice, we initialize \mathbf{x} from uniform distribution, and update \mathbf{x} by

$$\mathbf{x}^k = \mathbf{x}^{k-1} - \eta \nabla_{\mathbf{x}} E(\mathbf{x}^{k-1}) + \omega,$$

where $E(\mathbf{x}^k - 1)$ is the function that can measure the distance between \mathbf{x}^{k-1} and the real local distribution. $\omega \sim \mathcal{N}(0, \sigma)$.

In practice, we generate 50-100 samples of each local data set and add them to the current local data sets for training. However, because of the low quality of the generated data, the improvement is limited. Besides, the generated data will pollute the batch normalization(BN) layer, and we should use real data to refresh BN layer at the end of each round.

Core Set Methods. Another simple yet effective treatment in CL lines in the category of Exemplar Replay (Rebuffi et al., 2017; Castro et al., 2018). This approach stores past core-set samples (a.k.a. exemplars) selectively and periodically, and replays them together with the current local data sets. We tried two sample methods. First is so-called Naive method, in which the samples are uniformly chosen from local data sets. Except of naive select core sets, we also tried another core set sampling method introduced in iCaRL (Rebuffi et al., 2017). See Algorithm 3 for details.

In practice, we save 100 figures of each local data set and combine them with the current local data sets. Saving core sets perform best compared with these three approximation methods; however, only valid when the number of clients is limited.

C.1.3 Additional Experiments

Applicability of different algorithms. We list the applicability of different algorithms under various time-varying scenarios in Table 8.

Overlapping local data sets. We further relax the difficulty of federated continual learning, from challenging non-overlapping time-evolving heterogeneous data (e.g. in Table 4 and Table 5) to a moderate time-evolving case (i.e. the local data evolves with the overlapping, while the size of local data sets stay unchanged). Table 9 illustrates the performance of FL baselines and CFL methods, under different degrees of overlapping (the construction details refers to Appendix C.1.1): *the improvement of CFL methods is consistent to our previous results, while the overlap parameter has no obvious connection with the final global test performance.* We believe that both the overlap degree and the new arriving data influence final performance, and we leave future work on realistic time-evolving FL data sets to gain a better understanding.

Convergence curves for different settings. Figure 5 show convergence curves of CFL and FedAvg on different data sets. The settings are the same as results in Table 5. Models are trained on partitioned data sets with $\alpha = 0.1$, and all data

| Overlap | FL baselines | | CFL methods | |
|---------|--------------|--------------|---------------------|--------------------|
| | FedAvg | MimeLite | CFL-Core-Set | CFL-Regularization |
| 0% | 80.66 ± 0.40 | 80.78 ± 0.07 | 84.87 ± 0.11 | 81.27 ± 0.38 |
| 25% | 80.16 ± 0.01 | 80.17 ± 0.11 | 84.66 ± 0.11 | 80.67 ± 0.27 |
| 50% | 79.97 ± 0.23 | 80.35 ± 0.39 | 84.59 ± 0.07 | 80.91 ± 0.25 |

Table 9: Benchmarking FL baselines and CFL methods on different degrees of local data set overlapping, for training ResNet18 on split-CIFAR10 data set. The overlap reduces the degree of non-iid-ness. In order to observe a noticeable performance difference, we use a larger data distribution gap between rounds (i.e. $\alpha = 0.1$).

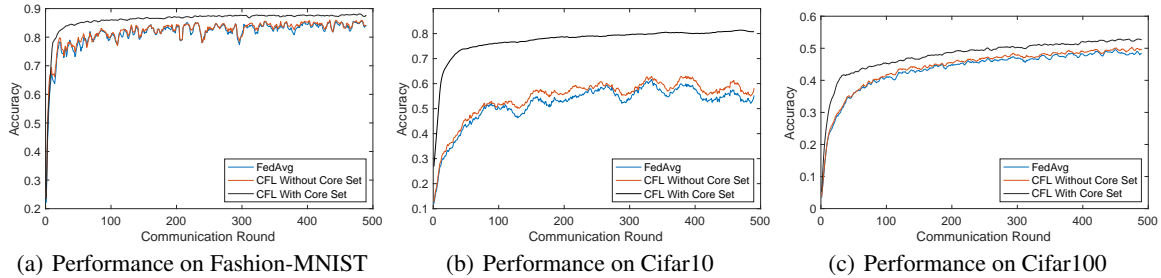


Figure 5: Models are trained on various data sets with $\alpha = 0.1$. CFL Without Core Set method use regularization methods, and CFL With Core Set methods use core set methods. All these two CFL algorithms use FedAvg as backbone.

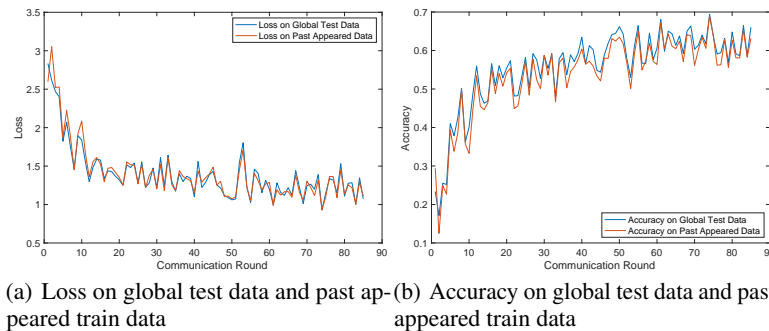


Figure 6: Evaluation on global test data and past appeared training data. We trained ResNet18 on split-Cifar10 data set with $\alpha = 0.2$ for 85 rounds.

sets are partitioned to 210 subsets for 7 clients. To show the difference between different algorithms more clearly, all curves are smoothed by a 1D-Mean-Filter. Results show CFL can converge to a better optimum compare with FedAvg.

Investigating resistance of CFL to time-evolving scenarios. Figure 7 shows the loss curve of CFL-Regularization and FedAvg on different data sets. Models are trained on partitioned data sets with $\alpha = 0.1$, and all data sets are partitioned to 210 subsets for 7 clients. The first column shows the loss curve of the first 300 rounds, and the second column shows the loss of some chosen details. Because of the non-iid-ness of local data sets, the loss will suddenly rise. Notice that *CFL-Regularization has an apparent mitigation effect on this situation.*

Difference between training and test loss. Figure 6 show the loss on global test data and past appeared training data. We evaluate the model with stateful clients, set $\alpha = 0.2$, and use FedAvg algorithm. We show that *there is no significant difference between loss value on global test data and past appeared training data.*

C.2 Algorithms

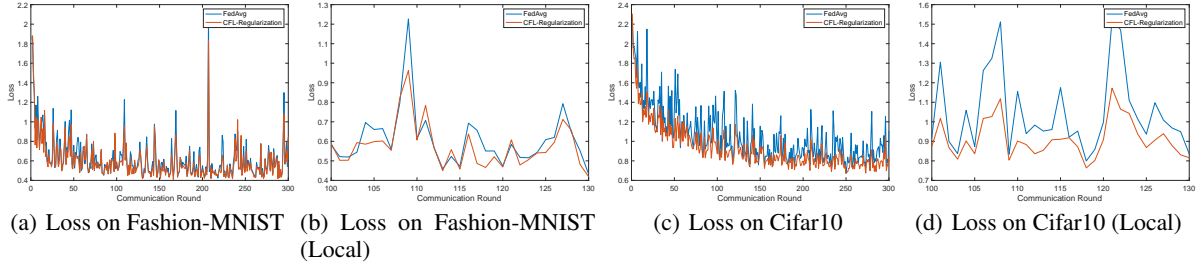


Figure 7: Models are trained on split-Fashion-MNIST and split-Cifar10 data sets with $\alpha = 0.1$. The loss is evaluated on global test data sets. Left column is the full curve of 300 rounds, and figures in right column are partially enlarged curves.

Algorithm 4 SplitdataMain

Require: S : total data set split by class, T : rounds, K, N, α, β

Ensure: D_{final} : split data set

```

1:  $D \leftarrow \text{splitData}(S, K, N, \alpha)$ 
2:  $D_{final} \leftarrow []$ 
3: for  $i = 1, 2, \dots, K$  do
4:    $S_i \leftarrow \text{splitByClass}(D[i])$ 
5:    $N_{local} \leftarrow \text{len}(D_m)/T$ 
6:    $D_i \leftarrow \text{splitData}(S_i, \text{cluster\_num}, N_{local}, \beta)$ 
7:    $D_{final} \leftarrow D_{final} \cup D_i$ 

```

Algorithm 5 renormalize

Require: θ : weights for different classes, i : the class that should be deleted

Ensure: θ : renormalized weights

```

1: for  $j = 1, 2, \dots, \text{len}(\theta), j \neq i$  do
2:    $\theta[j] \leftarrow \theta[j]/\text{sum}(\theta/\theta[i])$ 

```

Algorithm 6 Data splitting

Require: S : a list of data sets split by labels, M : the number of clients, N : the size of local data sets, α : the Dirichlet distribution parameter

Ensure: D : split data sets

```

1:  $D \leftarrow []$ 
2:  $G \leftarrow [0, 1, 2, \dots, \text{len}(S)]$ 
3: for  $m = 1, 2, \dots, M$  do
4:    $p = [p_1, p_2, \dots, p_{\text{len}(S)}]$ , where  $p_{t,i}$  denotes the fraction of class  $i$  in total data set.
5:    $\theta \leftarrow \text{Dirichlet}(\alpha, p)$ 
6:    $D_m \leftarrow \emptyset$ 
7:   while  $\text{len}(D_m) < N$  do
8:      $i \leftarrow \text{multinomial}(\theta, 1)$ 
9:      $y \leftarrow G[i]$ 
10:     $\text{data} \leftarrow \text{uniform}(S[y])$ 
11:     $D_m \leftarrow D_m \cup \{\text{data}\}$ 
12:     $S[y] \leftarrow S[y]/\text{data}$ 
13:    if  $\text{len}(S[y]) == 0$  then
14:       $G \leftarrow G/y$ 
15:       $\theta \leftarrow \text{renormalize}(\theta, i)$ 
16:     $D.append(D_m)$ 

```
